HYBRID FOAMED CO-INJECTION MOLDING

By

KAREN ROGERS

A Thesis

Submitted to the School of Graduate Studies

In Partial Fulfillment of the Requirements

For the Degree

Master of Applied Science

McMaster University

MASTER OF APPLIED SCIENCE (2008) McMaster University

(Chemical Engineering) Hamilton, Ontario

TITLE: Hybrid Foamed Co-Injection Molding

AUTHOR: Karen Rogers

B. Eng. (McMaster University)

SUPERVISOR: Dr. Michael Thompson

Dr. Andrew Hrymak

NUMBER OF PAGES: XIII; 68

Abstract

This project examines the co-injection molding of a TPO material, using a solid skin, and a microcellular core material. For useful industry applications, the density, and the tensile and flexural mechanical properties were examined, and compared to a solid injection molded TPO plaque achieve using different processing parameters and materials. Coreespondingly, the foam structure was examined to determine structural effects on the final mechanical properties. It was discovered that density can be reduced by as much as 32.0% ± 0.8%, while still maintaining mechanical properties comparable to those of a similar part using a solid material for the core. Elliptical cellular shapes and cells distributed more widely in the gap direction corresponded with lower density parts, yet maintained mechanical properties similar to higher density foams with circular cells concentrated along the center of the gap direction.

Fracture initiation was examined to determine if failure occurred within the foam structure of the parts, or the foam/core interface. Observations indicate that failure depended on the type of force applied to the part, as well as the material used to form the part itself.

ACKNOWLEDGEMENTS

I would like to express my most sincere thanks to:

Dr. Michael Thompson and Dr. Andrew Hrymak, my supervisors, who provided me with their guidance throughout this project.

Ms. Elizabeth Takacs, lab manager of MMRI, for her training and insight throughout this project.

Decoma, NSERC and AUTO 21 for their financial assistance through this project.

The Polymer Processing Group at McMaster for their help and support throughout this project.

My parents, Jan and Jack Rogers, sister Shelley Rogers, Kristin Davies and Matthew Whiteman for their continued support "from the beginning".

Table of Contents

Table of Figures

List of Tables

Chapter 1. Introduction

Co-injection molding (or two component injection molding) is a technology that was developed over 30 years ago; however, it is not yet a common practice in the plastics industry. In many ways, co-injection molding is the way of the future, especially for parts with foamed polymer cores. Recycled plastics can be used as core material, while maintaining the sharp, smooth image of a part made completely from virgin plastic. Inert gases can be used in the process to foam the material in order to reduce weight, resulting in an operation with a reduced environmental footprint, and a more economically molded product.

Foaming of polymer is an interesting way to decrease weight for many plastic parts. In the case of the automotive industry, this is crucial. Unfortunately, the surfaces of foamed parts are sometimes not aesthetically pleasing, and most buyers are interested in having a car bumper that appears smooth and shiny (i.e Class A finish). This is where

co-injection molding with foamed cores can be useful, being capable of producing a hybrid part with a smooth skin surface and acceptable weight reduction.

The optimization of this process is quite complex. In conventional injection molding, factors of interest for optimization include melt and mold temperatures, injection pressure, injection velocity, and shot volume of material. Many of these factors are inter-related, and can take much time and waste product to optimize. Co-injection molding processes nearly double the number of significant processing factors, as both plasticating units must be considered as well as any interactions as the two materials impinge upon one another.

The research documented in this thesis was completed to determine if this process is applicable to the production of an exterior automotive part where weight, part properties (mostly mechanical) and aesthetics are all critically important to its end use. The objectives of this work are:

1. Identify input and output factors that are most important to optimize the process.
2. Determine how mechanical properties of the parts change with foam morphology. The co-molded part structure needs to be studied and potential negative impact minimized for this process to be considered feasible within the automotive industry.

Chapter 2. Literature Review

2.0 Opening Remarks

After considering some of the advantages of foaming, such as faster processing time, lower injection pressure, increased impact strength, and lighter part weight (Turng and Kharbas, 2004), it is clear that injection molding a foamed polymer has many advantages over solid parts. These properties of foams are well-suited to the advanced engineering needs of the automotive industry where economics, function, and legislation are found to drive the selection of materials and processes used to manufacture parts. For exterior parts such as the bumper fascia or the entire front-end module, molded foam parts would seem ideal but have been restricted in use due to their poor surface appearance. The surfaces of injection molded foams often appear swirled, and after painting can appear dull due to collapsed cells in the surfaces of these microcellular materials (Li and Isayev, 2003). As an emerging alternative technology for the

manufacture of foamed thermoplastic parts, co-injection molding can provide the same high gloss surface to a foamed part as if it were solid. A lighter 'Class A' molded part now becomes possible with this technology. In co-injection molding, the core material containing the foaming agent is covered with a skin of solid material as it enters the mold cavity. Co-injection is familiar to this industry, being considered as a possible technology for paint replacement which is another area of interest as it is much safer for workers and the environment (Keestra et al., 2006).

The process of co-injection molding with a foam core is very complex, involving many factors which make the process difficult to control and models do not yet exist to assist in predicting performance; simulation of co-injection molding are present in the current versions of some commercial software packages but are of limited use in foam applications. Melt temperatures and viscosities of the incoming skin and core materials to the mold, mold temperature, injection pressure, back pressure, shot size, and shot speed must all be optimized in order to achieve desired characteristics for a final part. In the foaming process, properties must often be traded off such as decreasing part density leads to a decrease in mechanical properties. The skin material will help maintain mechanical properties. Throne (Throne, 2004), found that the best way to maintain mechanical properties with the foamed core is for the core material to be evenly distributed through the part, allowing for a consistent skin thickness. Heat transfer is crucial to this process since the injected skin layer can insulate leading to higher temperatures in the gas-laden melt of the core. Since cooling is important in providing a suitably viscous matrix capable of supporting newly grown foam cells, higher

temperatures can cause cell coalescence in the foam, and as the cells grow larger many of the structural properties of the part decrease (Throne, 2004).

2.1. Foaming

As mentioned before, the advantages of a foamed part over a solid one for the same matrix material can be highly beneficial to a manufacturer, though the process can be difficult to control. Methods and models are being created by researchers in the field in an attempt to classify these systems, which will be reviewed in the following sections. Foaming can be broken into three stages: nucleation, bubble growth, and stabilization (Naguib et al., 2002).

During **nucleation**, nuclei of gaseous cells are formed in the polymer matrix. Temperature, pressure, and shear play roles in **nucleation**. Temperature is important when a chemical blowing agent (CBA) is used in order to reach its decomposition state. The viscosity of the polymer material which controls nucleation, is most sensitive to temperature. And both temperature and pressure parameters can cause the change in gas solubility within the polymer necessary for nucleation, though in processing machinery the latter factor is more easily changed quickly (Leduc and Rodrigue, 2005). Higher injection speeds will result in a larger pressure drop, and in turn, more potential shear stress within the mold. Shear is recognized as a contributor to nucleation but its effects are difficult to decouple from other processing parameters.

These newly formed cells grow and expand during the **bubble growth** stage. The longer the system remains in this stage, the larger the gaseous cells are allowed to grow. Taki et al (Taki et al., 2006) examined the bubble coalescence times in different

polypropylenes, and observed that the amount of time for cells to coalesce depended mostly on the capacity of the matrix to strain-harden; as strain-hardening increased, so did the time before coalescence occurred during cell growth. The duration of the bubble growth stage is greatly affected by the rate of quenching used by the processing method. If fast quenching occurs, less growth of the foam results with fewer, smaller gaseous cells than in the case of a slower quench rate (Sun et al., 2004).

Finally, in the **stabilization** stage the morphology will become "frozen" and no further expansion of the cells is possible. Ideally, stabilization occurs before cellular rupture or coalescence so that a fine, cellular structure is produced and mechanical properties remain closer to those of the matrix resin (Gosselin and Rodrigue, 2005). For semi-crystalline polymers, the rate of cooling in the stabilization stage will have a strong influence on the crystallinity of the formed part. A fast quench results in a lower amount of crystallization by the polymer and a brittle final product, which is not ideal for automotive applications.

Foams are generally classified according to their apparent density. Low density foams are suited to cushioning and insulation where as high density and microcellular foams maintain sufficient mechanical properties to be used in structural applications. Low density foams are in the order of 90% porous while high density foams are less than 50% porous. Microcellular foams tend to be 10-20% porous but their classification is more strictly applied based on their cell size and cell density rather than a bulk density value. Microcellular foams consist of cells less than 10 μm in diameter and have a cell density greater than 10^9 cells/cm^3 (Naguib et al., 2002). For porosities between 50-90%,

these materials are considered to be medium density foams and are not commonly prepared with polyolefins (Throne, 2004).

2.2. Composition of a Foam

The materials needed to prepare a foamed part include a suitably viscous polymer and a blowing agent. A blowing agent may be either a physical gas such as nitrogen or carbon dioxide, or a chemical additive which generates a gas as it decomposes. In the latter case, such blowing agents are divided between those which decompose exothermically (e.g.. azodicarbamide) and those which decompose endothermically (e.g. sodium bicarbonate). Sometimes, additional powders or fibers are be used to alter the viscosity and mechanical properties of the matrix and which may simultaneously act as nucleating agents to minimize the energy required to initiate foaming.

2.2.1. Polymer Matrix Properties

Several factors are considered when choosing a polymer for foaming. It is important that the polymer exhibit a high melt strength otherwise the matrix will not be able to support the extensional forces developed during cell growth and the cells will rupture or coalesce (Naguib et al., 2002). It is ideal for the polymer to exhibit minimal crystallinity because crystalline structures have very little allowance for gas solubility and diffusion within. Doroudiani et al (Doroudiani et al., 1996) observed that longer cooling times allowed for greater crystallization, and therefore decreased the foamability of the material compared to faster cooling rates which allowed more amorphous regions to remain present within the system. This indicated that less crystalline structures of the

same material could more easily contain gaseous cells due to fewer crystalline regions, which innately do not contain gaseous cells (Doroudiani et al., 1996).

As a gas-laden melt, the gas phase will affect the properties of the matrix. Qin et al (Qin et al., 2006) examined the rheology of thermoplastic polyolefins using an in-line rheometer on an injection molding machine. They observed that the viscosity of a TPO decreased by as much as 30% as gas was added to the system by a chemical or physical blowing agent. The lower viscosity means less energy is required to process the material and reduces the amount of viscous heating that occurs, but pressures in the system will also be reduced and this must be managed in order to control the forming foam structure. Naguib et al (Naguib et al., 2005) examined the crystallization of gas-laden polypropylenes by varying the polypropylene architecture and foaming additives, using both a normal and a high pressure differential scanning calorimeter. They found that the temperature of crystallization decreased with the addition of a blowing agent, and increased with the cooling rate.

2.2.2. Blowing Agent

Blowing agents come in two different types, chemical and physical. Physical blowing agents are usually carbon dioxide or nitrogen. They are injected into the system to create the foamed material. Since there are no byproducts, this is much more environmentally benign. The drawbacks of using a physical blowing agent are that the nucleating sites cannot be uniformly distributed, and in systems that are not continuous (i.e. injection molding), it is difficult to control the pump due to the start/stop requirements of the method. An example of this was demonstrated by Bravo and Hrymak (Bravo and Hrymak, 2005), who studied physical foaming using high pressure gas

injection into a special nozzle containing a set of static mixers and a shut off valve. They found that there were issues with pressure which limited injection speed and part-to-part foam consistency. Because of the similar semi-continuous nature of co-injection molding and the need to focus on processing variables without concern for part-to-part variability, physical foaming was not considered as a preferred approach to foaming for this thesis.

Chemical blowing agents (CBAs) react over a specific temperature range which results in released gas(es) being dissolved into the polymer matrix (Throne, 2004). There are two types of CBAs: exothermic and endothermic. Exothermic blowing agents usually result in a high gas yield, and a large heat of reaction. Endothermic blowing agents tend to have a slow rate of gas yield, which in turn decreases the amount of coalescence that can occur, as well as the time for bubble growth. Hence, both types of CBAs result in a reaction that is difficult to control (Zhou et al., 2000). In addition, the main gas type evolved by endothermic CBA, i.e. CO_2, has a greater tendency to lower the melt viscosity of the polymer because of higher melt diffusivity. For the purpose of co-injection molding with a foamed core material, endothermic CBAs are ideal because they lower the melt viscosity of the polymer and reduce coalescence, resulting in a finer foam structure. In comparison, exothermic CBAs increase the bubble growth time due to the extra heat created. Exothermic CBAs often form nitrogen or carbon dioxide when activated.

2.2.3. Nucleating Agents

Nucleating agents can be invaluable to foaming because they increase the rate of nucleation during the foaming process by lowering the activation energy through

heterogeneous nucleation of cells (Tatibouet, 2000). Some common additives that act in this manner include talc, titanium dioxide, clays, and carbon nano-tubes. In some studies, it has been observed that more gas absorption is possible for filled polymer systems compared to their neat counterparts. It is assumed that the nucleating agent creates preferred sites for gas to accumulate and form cells (Chen et al., 2001).

2.2.4. Presence of additional fillers and additives

Fillers are often added to polymers in the automotive industry (Lee, L. et al. 2005). Talc is commonly used, and was chosen for this project because of its ability to increase the stiffness of the composite material. It also acts as a nucleating agent, which can potentially increase the amount of foaming in the polymer. Elastomer are also added to a polypropylene matrix in order to increase its overall fracture toughness; with low concentrations of the elastomer in the matrix (i.e. <5 wt%) the material is referred to as an impact-modified polypropylene whereas with higher concentrations they are known as a TPO. The elastomer component used is commonly a polypropylene-polyethylene copolymer. Because the elastomer is less crystalline than polypropylene, nucleation is more likely to occur either in the elastomer phase, or between the elastomer and polypropylene phases. Jancar et al (Jancar and Dibenedetto, 1994) observed that when fillers were blended with an elastomer and a polymer, there was either perfect separation of the filler in the polymer and the elastomer was dispersed in the matrix, or the filler was completely encapsulated by the elastomer, and there were two-phase particles dispersed throughout the matrix. When the filler is a nanoclay such as those used in nanocomposites, the size of the elastomer phase is reduced due to the presence of the clay (Lee, H. et al., 2005).

2.3. Foam Injection Molding

2.3.1. Integral Foaming

Integral foam injection molding is a way to decrease the density of a structural part by adding a blowing agent to the polymer material. In this process, the surface will often appear to be swirled and textured due to cell rupture at the mold wall. Although the weight reduction is desirable, as in the case of a car bumper, the appearance is not aesthetically pleasing.

When creating an integral foam, back pressure must be high in order to ensure expansion of the polymer only occurs within the mold. The pressure drop that occurs in the path after the nozzle of the machine allows gaseous cell nucleation and bubble growth to occur. In order to keep the size of the gaseous cells uniform, the polymer is injected at a fast rate so that bubble growth occurs consistently throughout the part (Villamizar and Dae Han, 1978). The pressure created by the expanding foam can act as packing pressure, and therefore, foamed parts are often noted for their excellent dimensional stability. Finally, for a consistent cell structure in the gap direction of a part, fast cooling is required to prevent large cells along the center of the part (Gong et al, 2005).

2.3.2. Co-injection Molding

There are two different types of co-injection molding: simultaneous and sequential (see Figure 2.3.1). Sequential co-injection involves injecting skin material (A) mold, followed by a shot of core material (B). Often, a second shot of skin material is injected into the mold for an A-B-A injection. Simultaneous co-injection involves

injecting both the skin and the core material at the same time, taking advantage of fountain flow.

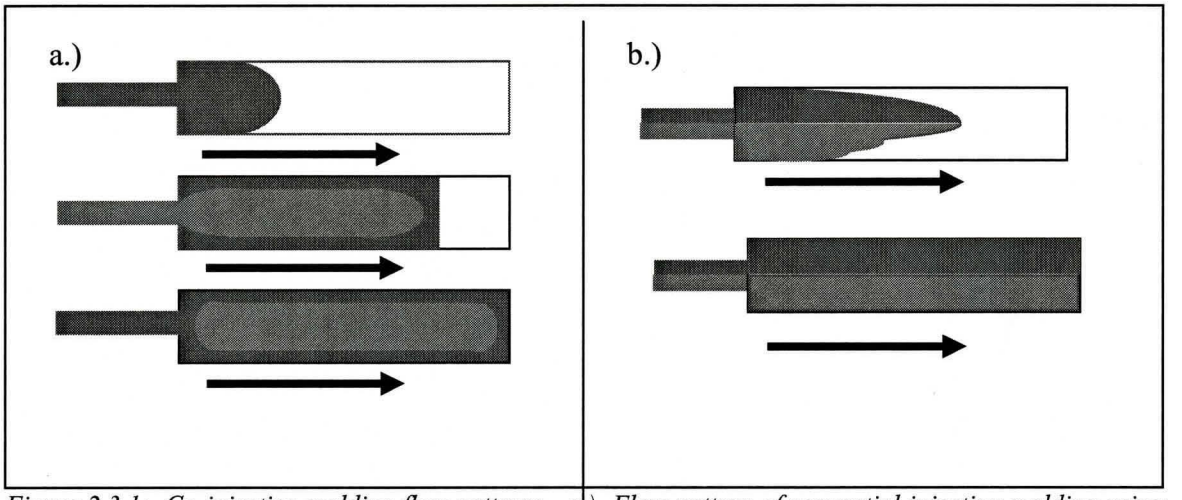

Figure 2.3.1: Co-injection molding flow patterns. a.) Flow pattern of sequential injection molding using A-B-A injection b.) Flow pattern of simultaneous injection molding using two materials.

Both simultaneous and sequential injection molding have significant advantages. They can assist in combining the properties of two different types of plastics. They can be used to make the surface of the material aesthetically pleasing while containing a foamed material, or recycled material. Other advantages of co-injection molding with a foamed core include shorter cycle times, a lighter weight part, low injection pressure, and better dimensional stability (Turng and Kharbas, 2004).

Considerations in co-injection molding must be made for the surface appearance. Watanabe et al (Watanabe et al., 2003) studied the flow behavior of simultaneous and sequential injection molding using a spiral shaped mold (analyzing the flow path around bends in the mold). They determined that in order to minimize the skin thickness of a part, and increase the core thickness, sequential injection was ideal. Because of fountain flow effects (which will be discussed in the next section), simultaneous molding was very difficult to optimize.

2.3.3. Fountain Flow

Fountain flow refers to how liquids decelerate when they encounter an interface moving at a slower rate, and spill towards the outer regions of the flow area (see Figure 2.3.2) (Mavridis et al, 1986). Mavridis et al (Mavridis et al, 1988) studied the impact of fluid dynamics during mold filling on the molecular orientation of a final part. They found that flow affects the molecular orientation more than temperature. They observed that as a part cooled the stress on the solid-liquid interface increased. They also found complex shear and elongation at the flow front.

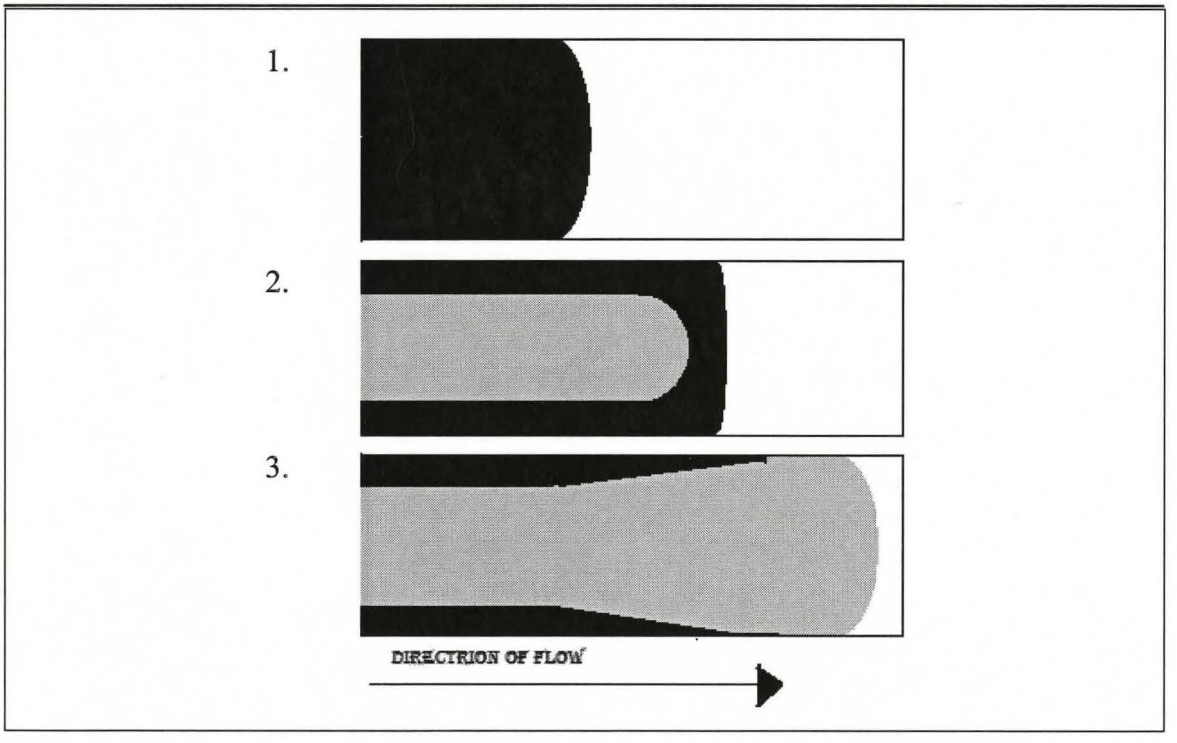

Figure 2.3.2: Fountain Flow in Co-injection molding.

Chen et al (Chen et al., 1996), studied polymer flow in the filling and post-filling stages of sequential injection molding. Their mold was a spiral shape, in order to estimate asymmetrical flow. Chen found that fountain flow dominated the flow in the mold. Fountain flow was observed because the skin (A material) thickness decreased

throughout the mold because of fountain flow. In fact, in regions with high packing pressure, the core material pushed through the flow front. This resulted in core material filling the entire thickness of the part in areas furthest from the injection point.

2.4. Processing Parameters Affecting Injection Molded Foams

Injection molding is one of the more popular methods used to process foam parts. This process has many factors to optimize, and there is much correlation between variables and observations. Barrel temperature, pressure, foaming agent concentration, injection speeds, mold temperature, and packing pressure all need to be considered in foam injection molding.

Desired characteristics of the foam parts used for this project include: smooth, class A surface appearance, density reduction of 20-25%, and as little decrease as possible in mechanical properties for the parts. In order to achieve these characteristics, the foam structure likely should contain a maximum of smaller cells per unit volume, allowing maximum weight reduction with minimal stress concentrators present and micro crack hindrance once failure occurs. Sequential injection molding was selected for this project due to the use of a lower viscosity gas-laden melt for the core of the part; the following considerations will cater toward sequential injection molding.

Park and Cheung (Park and Cheung, 1997) used injection molding and observed the effects of various parameter changes. They found that more uniform cells in foams that were produced at higher injection rates. The occurrence of coalescence was reduced and general cell size was smaller in parts that were injection molded at high temperature and low pressures. They also observed that when a nucleating agent was used, the foam had a finer cell structure, likely because the foaming agent had many more possible sites

to nucleate, spreading out the cells to slow coalescence. Because of these results, injection speed of all three stages as well as the melt temperature of the skin and the core materials are used as variables in the experimental design of this project.

Villamizar and Dae Han (Villamizar and Dae Han, 1978) studied the kinetics of bubble growth during injection molding. They found that mold temperature, injection pressure and the concentration of blowing agent had the greatest effects on the bubble growth rate. It was observed that increasing the melt temperature, blowing agent or mold temperature increased the bubble size, but the bubbles were not uniform in size or distribution. These results again indicate that temperature and therefore heat transfer was crucial in foaming, and all aspects of it should be examined. Heat transfer will be of concern in our process due to the insulating properties of plastic. Blowing agent is also important, as more blowing agent can result in more potential sites for cells to form and greater absorbed gas concentration in the matrix to participate in bubble growth. However, there is an upper limit to useful blowing agent content based on the solubility of the gas in the polymer during injection molding. A system must not be oversaturated with gas else when pressure decreases in the mold else large gaseous pockets will form (Xanthos and Dey, 2000). Additionally, higher CBA contents leave unacceptable levels of byproducts in the polymer.

Initiation of foaming is thermodynamically driven, being most sensitive to rapid changes in pressure or temperature. Since changes in temperature are slow for polymers, pressure and pressure release rate tends to play the most critical role in the nucleation of the foam. If the pressure is high enough, the polymer/gas matrix will exist in one phase until a pressure drop occurs. This pressure drop can occur anywhere, but ideally it should

occur as the solution enters the mold cavity. While pressure is the thermodynamic initiator of foaming in most cases, the rate at which the pressure drop determines the number of cells and overall cell size that can be formed. A faster pressure drop is more likely to cause simultaneous nucleation of all cells, which results in a large density of very fine cells for the final material. With all cells nucleated at the same time, less gas is available for any individual cell to grow. Shear is another process variable which has been linked to foam nucleation; however, it is difficult to separate its influence from other parameters changing in the system as the same time. Indirectly, shear mixing contributes to the gas distribution in the system, allowing maximum solubility. In this regards, injection speed is an important variable of study in this work, affecting both shear rate as well as the filling time of the process (Simha and Moulinie, 2000).

Hold time is another important parameter for examination in this work. Shorter hold times can potentially result in inadequate cooling, and the sudden pressure drop could result in potential distortion of the parts if the bubble growth stage is still occurring. Long hold times can ensure that the foam has reached the stabilization stage before being ejected (Simha and Moulinie, 2000).

The final parameter that was altered was the percentage of core material that composed the part, while the skin material amounts were kept constant. This parameter would result in various pressures within the mold, which could effect the cell nucleation within the foam structure (Simha and Moulinie, 2000).

2.5. Features of Foamed Parts

2.5.1 Shrinkage and Warpage

Shrinkage and warpage must be minimized in injection molded parts. Kramschuster et al (Kramschuster et al., 2005) studied the effects of processing conditions on shrinkage and warpage for microcellular and solid injection molding. They found that the amount of gas and injection speed affected the shrinkage and warpage of microcellular parts the most, while the pressures and times selected for the packing and holding stages affected solid injection molding the most.

Generally, a feature of foamed parts is a decrease in shrinkage and warpage due to the homogeneous packing pressure of the parts as a result of the bubble growth stage of the process. Shen et al (Shen et al., 2006) examined shrinkage and warpage in co-injection molded parts, and observed that the amount of blowing agent and the core-to-skin volume ratio had the greatest effects, indicating that a balance of core foam structure must be made with the skin encapsulating it.

2.5.2. Surface Defects

Surface defects such as *tiger striping* can occur when there is instability in the flow of polymer that is being extruded or entering a mold. Bogaerds et al (Bogaerds et al.,2004) used the Pom-Pom model to capture viscoelastic effects such flow instabilities in an injection molding process. They found that strain hardening decreased surface defects. They claimed that tiger striping was related to the elastic nature and rheology of the polymer. The more highly recoverable shear strain polymers were observed to have fewer defects.

Other potential surface defects to be considered for co-injection molding could be the result of the core breaking through the skin as a result of fountain flow. This would result in the surface appearing swirled or textured close to the ends of the mold due to the absence of solid virgin polymer.

Chapter 3. Experimental

The following section gives details on the materials, processing, and types of analysis used to examine the effects of co-injection molding parameters on the foaming of a TPO part.

3.1 Materials

The materials chosen for these experiments were a polypropylene with an MFI of 12 supplied by Ashland (HiVal PP HP 2420NA), Engage Elastomer (Engage 8407) supplied by Dow Chemical, and talc powder supplied by Luzenac (14807-96-6). The foaming agent was Hydrocerol HK40E (Clariant), supplied in masterbatch form. Finally, for comparison, a TPO nanocomposites supplied by Basell (Basell DX277AC) was used.

The majority of experiments were conducted with an in-house prepared thermoplastic polyolefin (TPO) which was created in a 27mm Leistritz twin screw extruder. The extruder was operated at a screw speed of 200 RPM, using a flat barrel temperature profile of 200°C, and a total feed rate of 20kg/h. Two different TPOs were

prepared, the first was a 70wt% polypropylene/30wt% elastomer blend (see viscosity curve in Figure 3.1.1), while the second was 67wt% polypropylene/ 23wt%elastomer/10wt% talc powder compound. The polypropylene and elastomer were tumble blended and fed by a gravimetric feeder. When talc was added, a side feeder was used in the configuration. To visually differentiate the skin and core layers in the molded structure, a colourant, specifically T-13 Rocket Red was used, which was supplied by DayGlow. The colourant was melt-mixed with the polypropylene in a Haake Rheomix 3000 batch mixer at a ratio of 90wt% polypropylene/10wt% colourant to make a master-batch. The mixer operated at 200°C with a rotor speed of 50 RPM for 15 minutes.

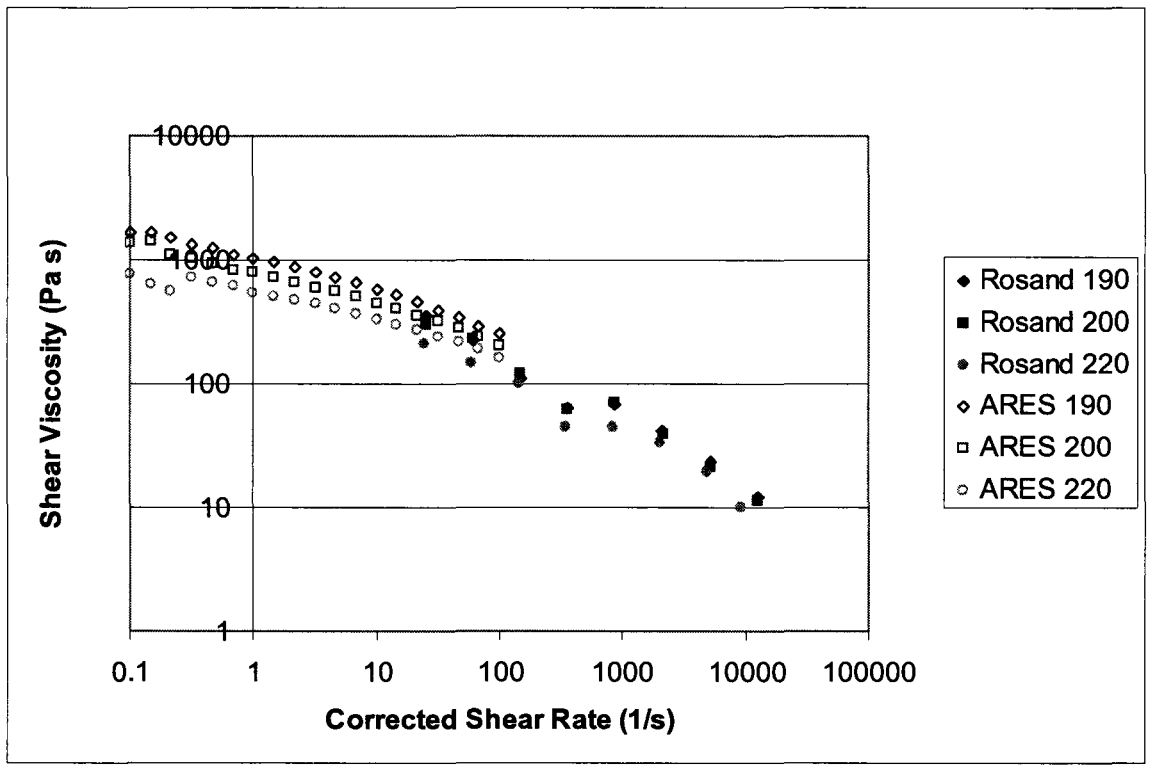

Figure 3.1.1 Viscosity curve for the 70wt% polypropylene/30wt% elastomer blend

3.2 Processing

The co-injection molding machine for this study was an Arburg Allrounder 320S injection molding machine. For co-injection purposes, the machine has two plasticating units, the main unit is mounted horizontally for in-line injection while the secondary unit was mounted vertically. An interval platen controlled the flow of the two units entering the mold. The machine has a 55 ton clamping capacity.

An ABA co-injection sequence was used, injecting a shot of skin material (A), followed by core material (B), and then a second shot of skin material (A) to fill the sprue. For an experiment, the core and skin materials were the same polymer; however, only the core material contained blowing agent in these experiments. The mold was a plaque with dimensions of 125 mm (width) by 100 mm (height) by 3mm (in gap thickness). The direction of injection was parallel to the gap dimension at the center of the mold area.

Table 3.1: DOE for TPO Plaques

	Skin Temp	Core Temp	Injection Speed 1	Injection Speed 2	Injection Speed 3	Hold Time	Percent Core	Mold Temp	Conc. Foaming Agent
	1	2	3	4	12	23	13	24	14
1	220	220	100	100	100	30	80	70	5
2	200	220	100	100	60	30	75	70	1
3	200	220	100	100	60	5	80	30	5
4	200	200	100	100	100	5	75	30	1
5	220	220	60	100	100	5	75	70	5
6	200	220	60	100	60	5	80	70	1
7	200	220	60	100	60	30	75	30	5
8	200	200	60	100	100	30	80	30	1
9	220	220	100	60	100	30	80	30	1
10	220	200	100	60	60	30	75	30	5
11	220	200	100	60	60	5	80	70	1
12	200	200	100	60	100	5	75	70	5
13	220	220	60	60	100	5	75	30	1
14	220	200	60	60	60	5	80	30	5
15	220	200	60	60	60	30	75	70	1
16	200	200	60	60	100	30	80	70	5
S1	220	220	100	100	100	30	80	70	0
S8	200	200	60	100	100	30	80	30	0

The different materials (in-house TPO, Basell TPO, and in-houseTPOtalc) were processed according to an experimental matrix which varied the temperature of the skin material, the core material, injection speeds, hold time, mold temperature, and concentration of foaming agent. In regards to the injected materials, the skin shot volume was held constant (8.25 cm^3) while the core volume was varied. Also, the second injection of skin material to fill the sprue was held constant at $1cm^3$. The experimental design of experiments (DOE) for the TPO material used a two-factor factorial design, and can be viewed in Table 3.1, while the levels of each variable can be observed in Table 3.2. A total of 16 runs were completed for each material, as well as an additional 2 runs which included a solid core (0% foaming agent).

Table 3.2: Levels of variables in DOE.

Variable	**Low Level**	**High Level**
Skin Temperature	200°C	220°C
Core Temperature	200°C	220°C
Injection speed: Skin, first shot	60 cm^3/s	100 cm^3/s
Injection speed: Core material	60 cm^3/s	100 cm^3/s
Injection speed: Skin, second shot	60 cm^3/s	100 cm^3/s
Percent Core material per shot	75vol%	80vol%
Hold Time	5 sec	30 sec
Mold Temperature	30°C	70°C
Concentration of Foaming Agent	1wt%	5wt%

The processing parameters were selected first by reviewing the literature. The temperature of the materials has been shown to be very important in foaming, so all temperatures were controlled. Values were selected to cover the common processing ranges for the materials. The mold temperatures were selected to span a wide range of temperatures. Injection speed can affect shear, pressure, and viscosity of the material, so it was varied in the experimental design. Hold times were selected to examine a range of times that would be time efficient in an industrial injection molding machine. The amount of core material was also selected after some preliminary trials. The low level for the concentration factor regarding the core material was found to be the minimum required to fill the mold whereas the high level was the maximum amount of material that could be injected without creating flash. The fixed amount of skin material was found to be adequate to cover the walls of the mold. The second shot of skin material was enough to fill the sprue of the mold. The foaming agent levels were again selected after preliminary trials. When more than 5% foaming agent was used, foaming was uncontrollable. The low value of 1% gives a range of foaming agent levels.

The TPO, TPOtalc and Basell materials were all processed and compared to further explore differences in single and co- injection molding, using solid and integral foam parts for the single injection molded plaques, and solid and foamed cores for the co-injection molded parts. The parameters for the single injection molded parts can be observed in Table 3.3, while the parameters for the co-injection molded parts are the same as Runs 1 and S1 in Table 3.1.

Table 3.3: Parameters for single shot injection molded plaques

	Material Temperature	Injection Speed	Cooling Time	Total Mold Volume	Mold Temperature	Concentration of foaming agent
Integral	200	35	5	45	30	5
Solid	200	35	5	45	30	0

Processing parameters for the solid and integral foam parts discussed in the "Main Four" Section.

3.3 Mechanical Analysis

In order to characterize the changes in the foamed parts with measures appropriate to the automotive industry, the selected response variables to the DOE trials were apparent density, foam cell size and locations, tensile modulus, tensile strength and flexural modulus.

3.3.1 Apparent Density

The apparent density of the parts was determined using the water displacement method. Three samples were measured for each run completed. Possible error can occur in these samples as a result of open cells present from cutting the samples to make them fit into the volume measuring apparatus. A band saw was used to make these cuts, so some of the cells potentially were closed off as a result of smearing.

3.3.2 Foam Structure

A optical microscope was used to determine the foam structure of the parts. The molded plaques were cut using a band saw parallel to the 125mm long edge, along the center of the part. A razor was used to slice specimens 4cm long, beginning at the edge furthest from the injection point. The sample was divided into four 1cm sections from

the edge farthest from the injection point (see Figure 3.3.1). These samples were then put under the microscope along with a slide that had a 1mm mark on it for a scale. Digital photos were taken, and then analyzed in SigmaScan Pro 3.0 (Jandel Scientific). The thickness of the skin layer, the distance from the outer edge of the part to the closest gaseous cell (*distance-to-cells)*, and the cell diameter (in the direction of flow) were measured. Cell shape was also examined qualitatively

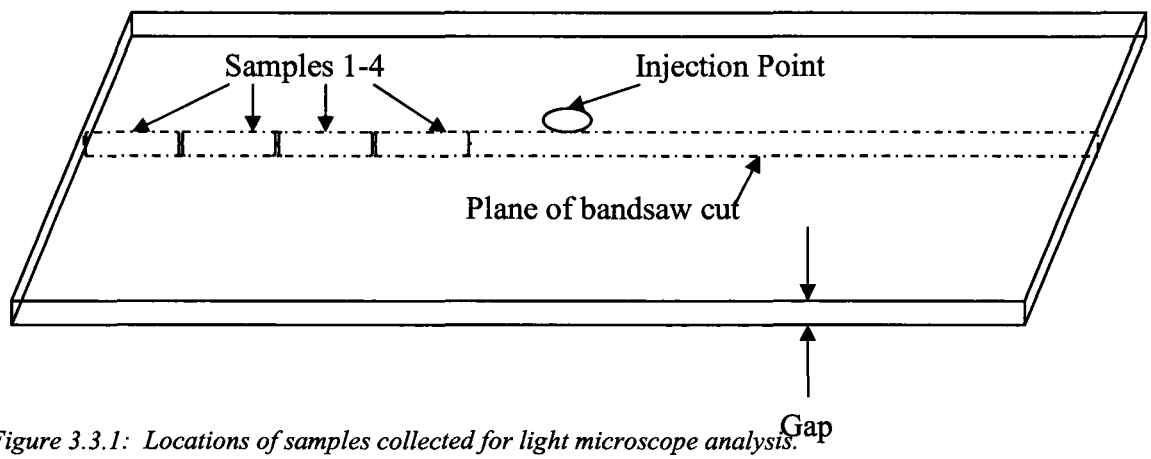

Figure 3.3.1: Locations of samples collected for light microscope analysis.

3.3.3 Tensile and Flexural Properties

Both tensile and flexural properties were measured using an Instron testing machine 3366 with a 5 kN load cell. Dog bone specimens cut according to ASTM Type IV dimensions were used for the tensile testing (focusing on tensile modulus and tensile break strength). Rectangular bars were used for the flexural testing (flexural modulus)

with a length and width of 8.2cm by 1.25cm, respectively supported on a span of 4.0 cm. Both tensile and flexural samples were cut from the TPO plaques using a hydraulic press. A sample was cut approximately 1.5cm from the edge of the part, and another was cut approximately 4cm from the edge of the part in order to determine if there was a significant change in properties. Both were cut perpendicular to the 125mm edge of the plaque (see Figure 3.3.2).

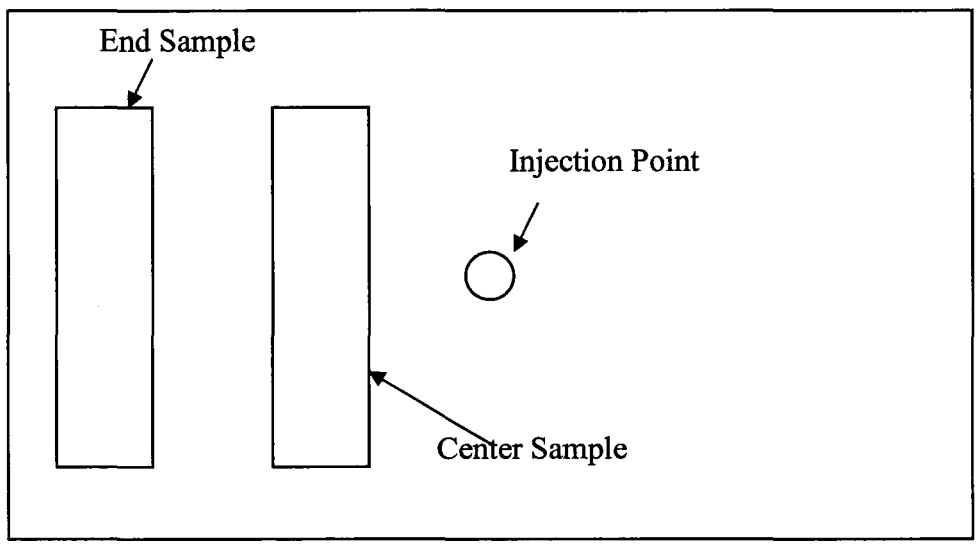

Figure 3.3.2: Mechanical analysis specimens. Locations of specimens punched from an injection molded plaque to be used for mechanical analysis.

Chapter 4. TPO Plaque Analysis

The analysis of this chapter was limited to the in-house TPO prepared without talc. The purpose was to observe the effects of different variables, and compare a co-injected foamed part with a solid part. Runs 1 and 8 were selected to be repeated to make comparative solid parts because Run 1 had all parameters at their high levels, while Run 8 had the maximum amount of low level parameters in the experimental design with all the temperatures and the amount of foaming agent at their low level values. As discussed in the literature review, temperature and the amount of blowing agent have been shown to be most influential on foaming. The densities of Runs 1 and 8 were at the high and low ends of all density values measured, indicating that they were good representatives covering the range of foam properties. Only two solid runs were completed because of a lack of material.

Fourteen of the sixteen co-injected parts (all runs with the exception of Runs 3 and 5) appeared visually the same as the solid injection molded parts, which met the

requirements of a part with a class A surface according to the criteria determined by GM. The two that did not fit these specifications were Runs 3 and 5, which expanded excessively in the gap direction creating an inflation effect, and a gap measurement much greater than that of the mold. This indicates that an optimized co-injection molding design is suitable for processes requiring a Class A surface appearance. The following sections will consider the physical changes to the co-injection molded parts, to determine if this processing method is an adequate substitute for injection molding.

4.1 Apparent Density

The goal of 25% material reduction by foaming for the TPO proved to be possible, and was even exceeded in some samples. The highest density reduction observed which maintained the shape of the mold was 32.0% ± 0.8%. The density reductions for each of the 16 runs are displayed in Figure 4.1.1.

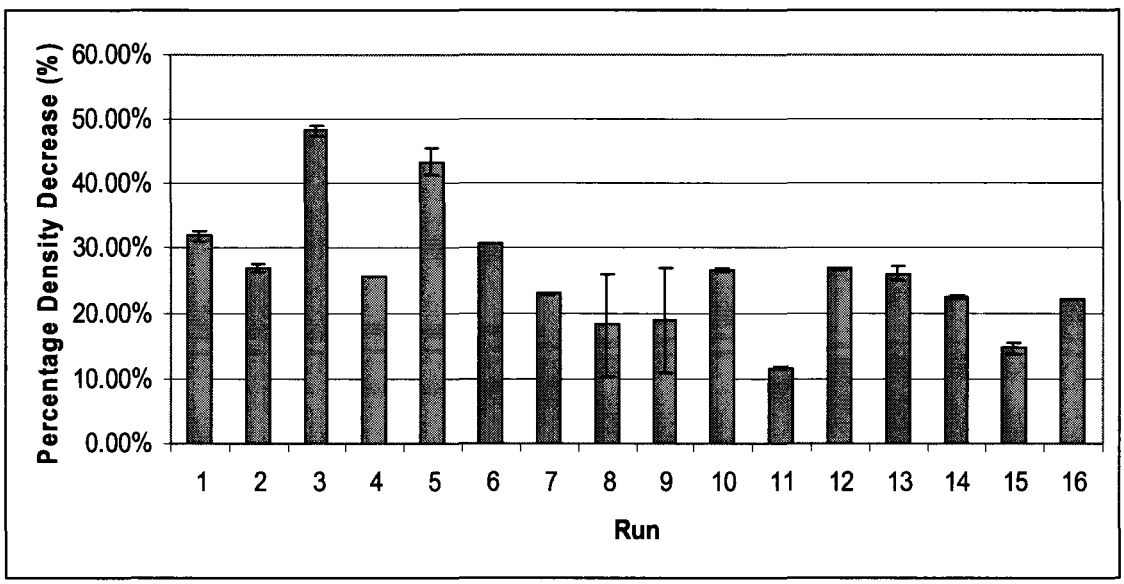

Figure 4.1.1: Apparent density reduction in TPO samples. Percentage reduction in density for the co-injection molded foam samples based on variation of processing conditions

Based on statistical regression analysis (see Appendix I) of the density data, it appeared that the factors of injected melt core temperature and the amount of core material* injected had the greatest influence on the density of the parts. With higher temperature and percentage of core material, more gaseous cells can nucleate and grow which results in a lower density plaque, and is consistent with most foaming papers examined in Chapter 2 (Naguib et al., 2002, Throne, 2004, Doroudiani et al., 1996, Naguib et al., 2005).

4.2 Microscope: Cell Morphology

Microscope work was completed following the procedure explained in Chapter 3. These results were compared with those of the density, tensile and flexural properties in order to relate morphology to physical properties.

4.2.1 Skin and Core Properties

The three values measured from the microscope analysis were the skin thickness, the distance-to-cells, and the cell diameter (Figure 4.2.1). The skin thickness was the thickness of the skin material, which contained no colourant, and was visually easy to observe. The *distance-to-cells* was the distance from the outer edge of the skin material (the surface of the part) to the closest gaseous cells. The cell diameter was the diameter of the cells in the direction of polymer flow (which was in the horizontal direction in all shown micrographs).

* The volume of skin material injected was held constant at 9.25cm^3, while the volume of core material was changed. The volume of core at the low level was 75% of the total volume of the part, and at the high level was 80% of the total value of the part. These percentages include the volume of gas injected.

The skin thickness between the different samples was consistent along the plane parallel to the direction of flow for each part (see Figure 4.2.2). The skin thickness was also statistically the same between runs (see Appendix II). The similarity in thickness showed that the core processing features dominated the part dimensions in this study. The through-plane distance from the outer surface of the skin and the closest cell, i.e. *distance-to-cells* (see Figure 4.2.2), was also consistent in the direction of flow for an individual run along the 5 cm length of part examined (see Appendix II). Unlike skin thickness, however, *distance-to-cells* did vary between runs (see Figure 4.2.2).

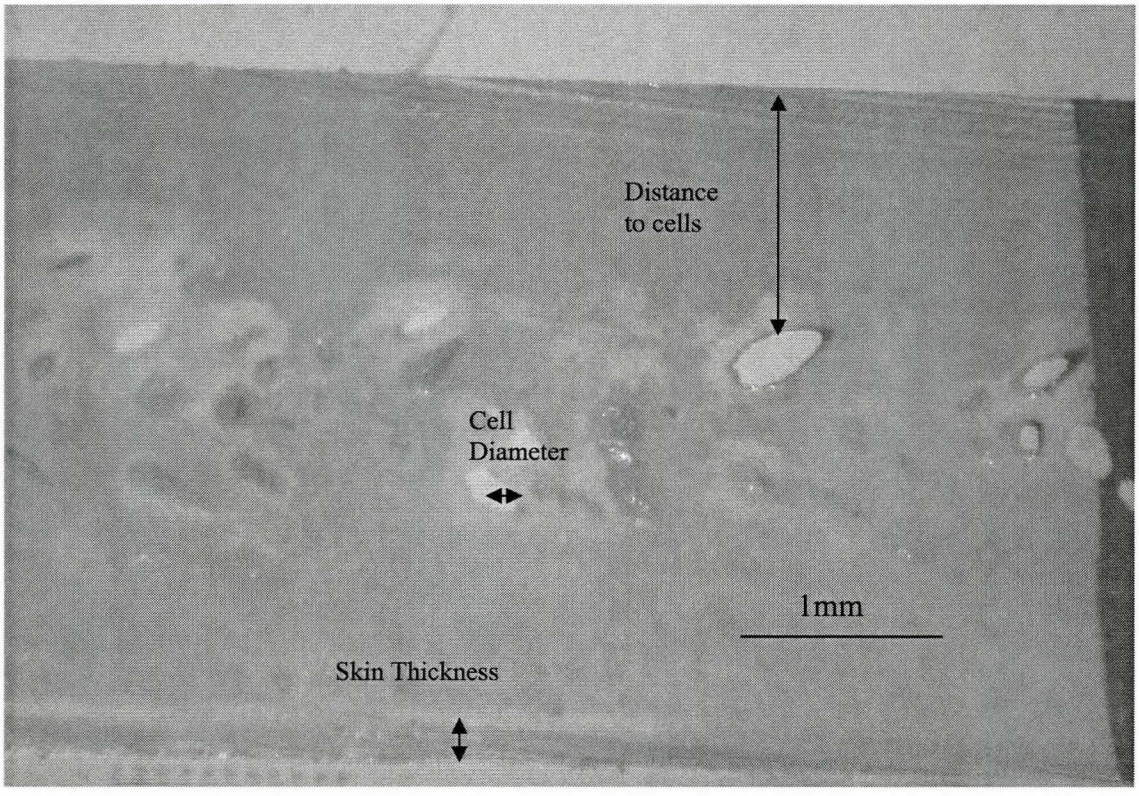

Figure 4.2.1: Micrograph from an optical microscope showing the measurement of skin thickness, cell diameter and through-plane distance to cell from a sample. The through-plane gap being the vertical axis, and the flow direction being the horizontal axis of the micrograph.

Runs 1 and 7 had the greatest *distance-to-cells* measurements of all the runs. Both had high level cooling times in the design of experiment. Run 5 had the smallest

distance-to-cells measurement, and lower level hold time, which is consistent with Runs 3 and 6, which also have low *distance-to-cells* measurements. Run 2 also had a low *distance-to-cells* measurement. The foaming agent and amount of core material values were low, and the mold temperature was high, so in this specific case, less cooling was required, and was likely adequate for the run. It appeared that the *distance-to-cells* measurement was mainly dependant on the cooling rate used for the part.

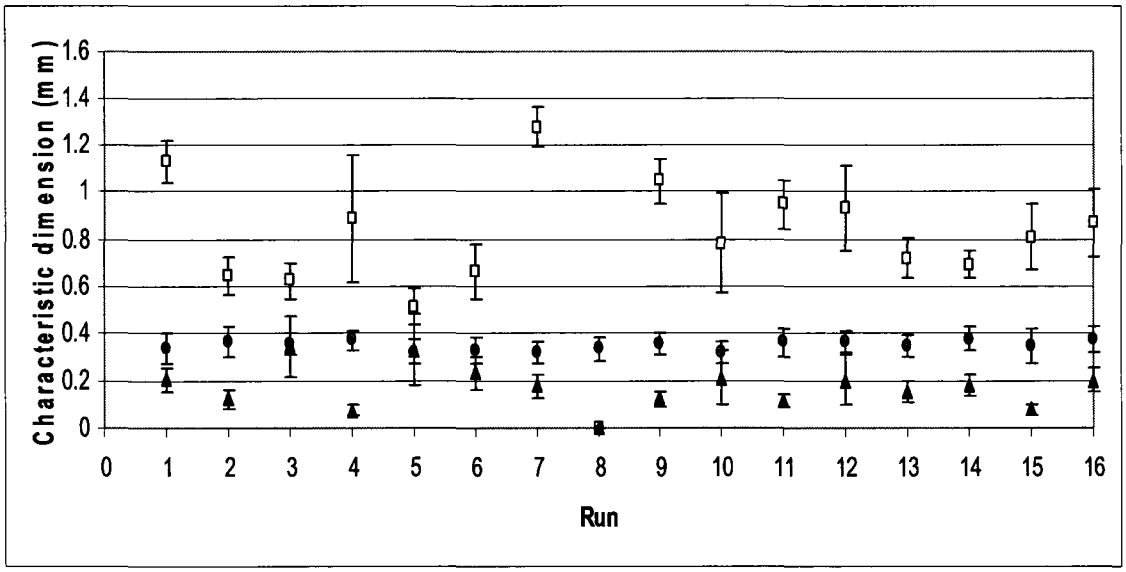

Figure 4.2.2: Microscope analysis of TPO plaques. Average skin thicknesses (●), distances to cells in the through-plane direction (□) and cell diameters (▲) in the direction of flow based on experimental conditions. Measurements taken over a 4cm length of part between the center and end. .

The cell diameters also differed between runs; however, were somewhat consistent in the direction of flow (see Figure 4.2.2). There were three types of cells observed in this work: circular (Figure 4.2.3a), elliptical (Figure 4.2.1), and extended planar voids which separated the part along the center of the gap (Figure 4.2.3b), which were observed for Runs 3 and 5, but not included in the cell diameter measurement. The

distance-to-cells and cell size were compared for each type of cell (Figure 4.2.4). The samples containing elliptical-shaped cells had a tendency to have a smaller *distance-to-cell* compared to samples with circular-shaped cells; the gaseous cells were not concentrated in the center plane of the gap, but rather throughout the gap direction. Because the parts with elliptical shaped cells had similar densities to some of the parts with circular shaped cells, while the parts with elliptical shaped cells had smaller *distance-to-cells* measurements, it is likely that the parts with elliptical shaped cells had greater distribution of cells within the thickness of the parts, which resulted in a greater distribution of potential stresses applied to the system. The maximum standard error in the *distance-to-cell* measurement was 30%.

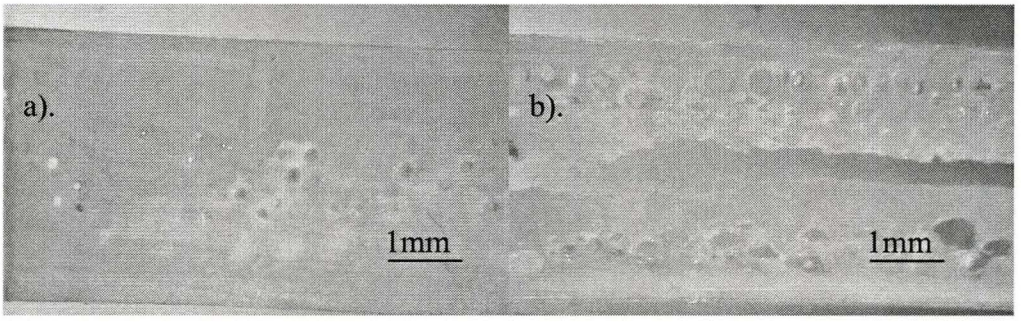

Figure 4.2.3: Microscope view of circular shaped cells and planar void. a) Micrograph of a part with circular shaped cells b) Micrograph of a part with a planar void along the center of the part

Considering the steps in foaming discussed in the literature review, the shape of the cell provided some insight into where cell growth occurred as the mold filled and how quickly heat transfer stabilized the resulting bubble before coalescence could occur. The elliptical-shaped cells corresponding to Runs 2, 10, 13 and 15 were likely a result of the bubble growth stage occurring while the material was exiting the sprue and entering the mold, experiencing the shear from the polymer flow, as well as mold walls and cooling material. Chen et al (Chen et al., 2002) studied foam nucleation under shear stress,

indicating that when nucleation occurred under shear, elliptical-shaped cells were formed, and the gaseous cell density was increased as shear was introduced, which indicated that the polymer began solidifying and crystallizing as injection occurred, when shear stresses were greatest. The circular shaped cells found in samples from Runs 1, 4, 6, 7, 9, 11, 12, 14, and 16 experienced cell growth once the molds had been filled, and there was no shear present. Interestingly, Runs 6 and 12 occasionally had elliptical cells located in the foamed core of the part close to the location of the *distance-to-cell* measurement locations. The cells located within the parts were a combination of cell types occurred occasionally (in 33% of the parts examined) for both Runs 6 and 12. As for the parts from Runs 3 and 5 which showed extended planar gaps in the center of the part, this was likely a result of inadequate cooling which allowed the bubble growth stage to continue after the part was ejected from the mold. These parts expanded in the gap direction, creating the planar gap.

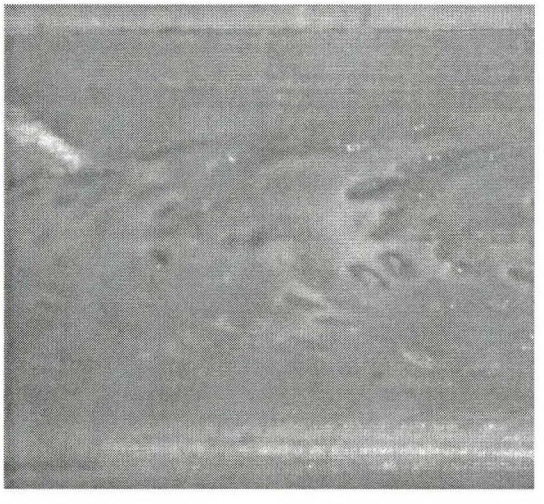

Figure 4.2.4: Microscope photo of plaque containing circular and elliptical shaped cells

The runs were divided into three groups, one for each cell classification, to determine common parameters within the experimental design which could provide

possible factors which contribute to each type of cell shape. The cell classifications are, "circular", "elliptical", and "planar separation". For the "circular" group, there were no common factors that appeared to lead to this specific shape. No patterns were observed, which indicated that a combination of parameters determined the circular cell shape; the circular cell shape occurred in 62.5% of the samples examined. The "elliptical" shaped cells appeared only for thosee conditions which used 75 vol% core material. The lower level of core material meant that the mold itself had a lower level of material within, resulting in more potential for gas expansion within the molded part. Although no other parameter was the same for the four runs with elliptical cells, three of the four runs also corresponded with use of the low level of foaming agent. All of the samples also had injection speeds of the core material and/or the second shot of skin material at low levels, resulting in a slower rate of injection. Since coalescence is time dependent, it is possible that the slower injection speed resulted in bubble growth occurring before mold filling had completed. Finally, the planar separation parts were examined. Both parts had high core temperatures, high speeds of core injection, short hold times, and high levels of foaming agent. The combination of high core temperature and high foaming agent allowed more potential nucleating sites and a slightly higher amount of cooling time, since more heat would need to be removed in order to reach the solidification temperature. The high speed of injection and short hold times resulted in less time for a plaque to cool and stabilize, which likely resulted in bubble growth continuing once the part had been ejected from the mold.

To conclude, it is apparent that cell shape is difficult to control, which follows, as foaming is also difficult to control. A combination of inadequate cooling and excess

nucleation and cell growth can produce an unacceptable part. Hold times appeared to affect the *distance-to*-cells measurement, relating to the cooling of the part. Elliptical-shaped cells found in some samples were likely related to the amount of material in the mold, and the rate at which it was injected. Circular-shaped cells are the most thermodynamically stable of the three cell shapes, and in the majority of cases, were formed in our experiments. When injection was within reasonable parameters, this is the most likely cell shape to be produced.

4.3 Mechanical Properties

While density reduction of molded parts may offer economic and performance advantages, meeting mechanical specifications is crucial for many applications like those found in the automotive industry. The two plaques showing the highest density reduction proved to have very poor mechanical properties, unable to meet the specifications of auto makers for bumper fascia moldings. Other runs showed only minor decreases in the mechanical properties measured, indicating that foam injection molding by sequential injection could still met the specifications required by industry and reduced material use as well. It is noted here that although samples were cut from two distinctly different region of the mold, i.e. close to the center of the plaque and close to the end of the plaque, the mechanical properties were comparable. When only one value is given, the center value is being reported.

The same two runs as in Section 4.2 were also repeated using a solid core in order to compare the mechanical properties of parts with foamed cores to those with solid cores.

4.3.1 Tensile Tests

Tensile testing was completed on the parts using the process discussed in Chapter 3. The focus of the analysis was on the break strength of the parts, and the tensile (Young's) moduli of the parts, which were compared to the density of the parts in order to establish a trend. It should be noted that there was whitening along the span of the parts due to the force of the punch used to cut the dogbone shaped specimens. This suggests that the tensile values may be lower than expected due to microcrack initiation during part preparation. However, the results should be comparative as all parts experienced the same amount of change during punching.

Break strengths (ultimate tensile strength) are displayed for each run in Figure 4.3.1, and are compared to apparent density in Figure 4.3.2.

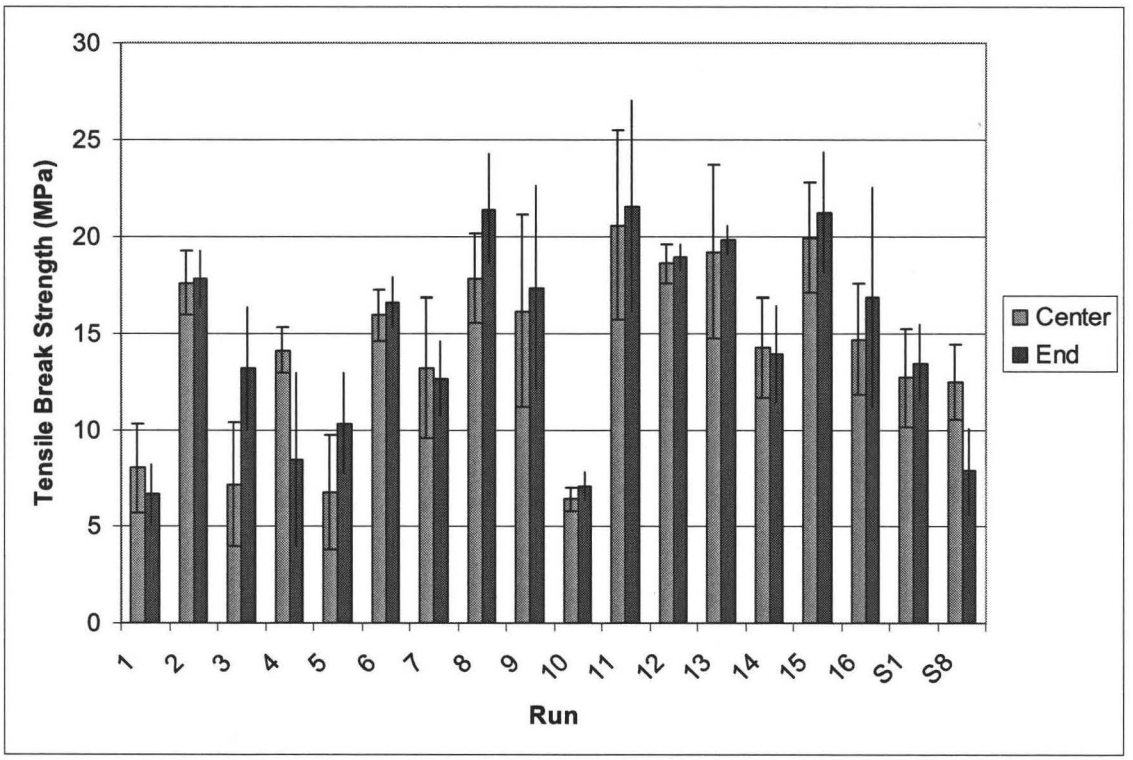

Figure 4.3.1: Break strength of each TPO run, completed from the dog bones cut close to the center and end of the part. S1 and S8 were molded using the same variables as Runs 1 and 8, except that they contain 0% foaming agent.

It can be observed that the difference in break strength between the center and the end of the parts is statistically the same in most cases. This indicated uniformity of the layer composition across the majority of the parts. The results showed that the tensile break strengths of the foam core parts were comparable to those of the parts with the same injection parameters and solid cores of the same material. In fact, in the case of Run 8, the foamed core part showed an increase in break strength over the version with a solid core (Run S8). Conversely, the foamed sample from Run 1 showed a lower break strength compared to its solid control (Run S1).

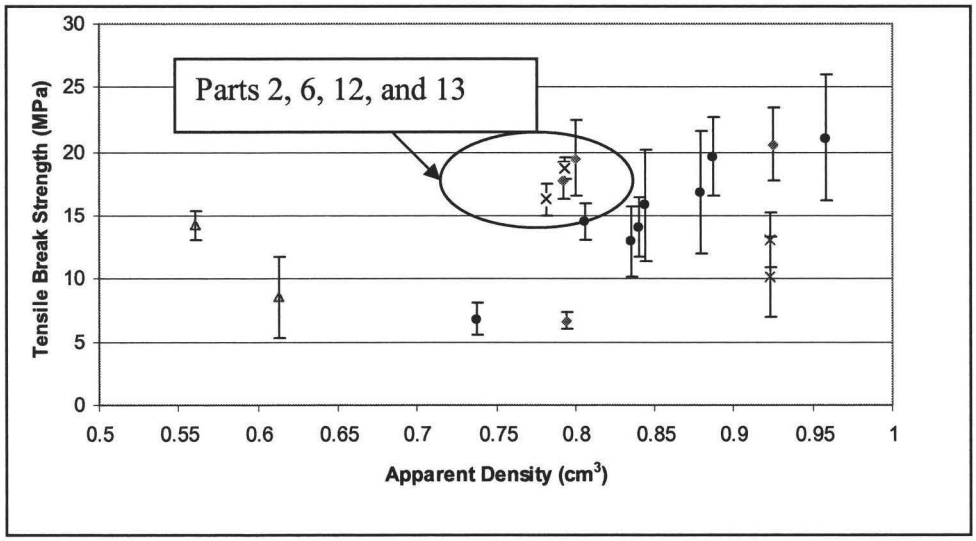

Figure 4.3.2: Tensile break strength of the parts compared to apparent densities. The parts with circular shaped cells (●), elliptical shaped cells(◉), a combination of circular shaped cells (x), planar separation, and solid parts(x) are compared.

There was no clear relation between tensile break strength and apparent density (see Figure 4.3.2); however, for higher density foamed parts the tensile break strength was notably greater than that of a co-injected part containing a solid core. Similarly, there was no correspondence of strength with the distance-to-cell measurement. This indicated that the cellular structure allowed the tensile force to disperse, absorbing the

energy, likely in the form of crazing, which can occur more readily within a foam structure. The cells likely also acted as crack arrestors, hindering potential failure initiations.

There are some interesting plaques which had densities between 0.75 and $0.8 g/cm^3$ that did not follow the trend of the other parameters. Specifically, these parts are Runs 2, 6, 12, and 13, which all had elliptical-shaped gaseous cells. Considering the great decrease in density for the parts with elliptical gaseous cells compared to parts with circular shaped cells, it was assumed that the core was more porous when the cells were elliptical. The elliptical-shaped cells likely transferred the tensile stresses applied to the system within the plaque as observed in Figure 4.3.2, distributing the stresses to the outer solid skin material, and the area between the outer skin and the cells.

It is clear that this theory would only be applicable up to a certain decrease in density. In the lower density parts, the break strength was low. Interestingly, the two lowest density parts (Runs 3 and 5) had break strengths similar to those of the plaques containing solid cores. The lowest density parts were the ones that experienced planar separation, and contained large cells. If failure occurred at the interface of the parts with solid cores, then it followed that after the initial failure propagated, the part acted as either two or three separate planes of material. Because of the great density reduction in the lower density parts, they also could have behaved as two parallel planes of material. This was possibly why the break strengths for these parts were comparable.

It follows for the lowest density part with circular cells (Run 1), which had a concentration of cells along the center plane of the part, observed in the *distance-to-cells* measurement for this part. The lowest density part with elliptical shaped cells (Run 10)

also experienced low average tensile break strength when compared to the other samples. The cell size, and the *distance-to-cells* measurements were both large in comparison to other parts with elliptical-shaped cells. The localized density reduction along the center of the plaques for Runs 1 and 10 would have acted as the location of fracture initiation, and the parts would then behave more like two parallel planes of material.

The tensile modulus was measured for the samples as well. A comparison of the tensile modulus for the parts cut from the centers of the plaques and the parts cut from the end of the plaques for each are shown in Figure 4.3.3, and a comparison of the center modulus values and density are shown in Figure 4.3.4.

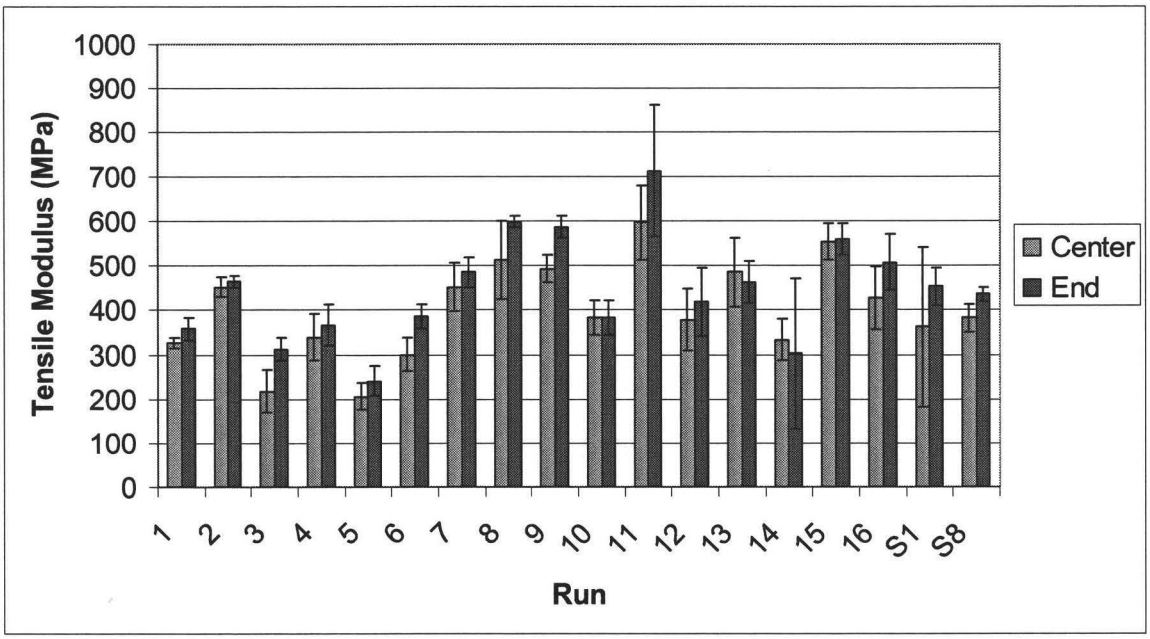

Figure 4.3.3: Comparison of the tensile moduli of TPO specimens. Measured from pieces cut close to the center of the TPO plaques and cut close to the end of the plaques. (S1 and S8 have solid cores, but the remaining processing conditions of Runs 1 and 8).

Similar to earlier discussed results, there was very little difference in the moduli of the test bars cut close to the center of the plaques, as opposed to those cut close to the end. Many of the runs had comparable properties to the solid parts. Runs 1 and 8

showed no statistical evidence of having moduli that were different from their solid core counterparts, Runs S1 and S8. Only those parts with apparent density reduction over 40% showed a decrease in tensile modulus of up to 45% compared to the solid parts.

When comparing the apparent densities of the plaques with the tensile moduli of the pieces cut closer to the center of the plaques, a weak parabolic relationship was observed, (Figure 4.3.4).

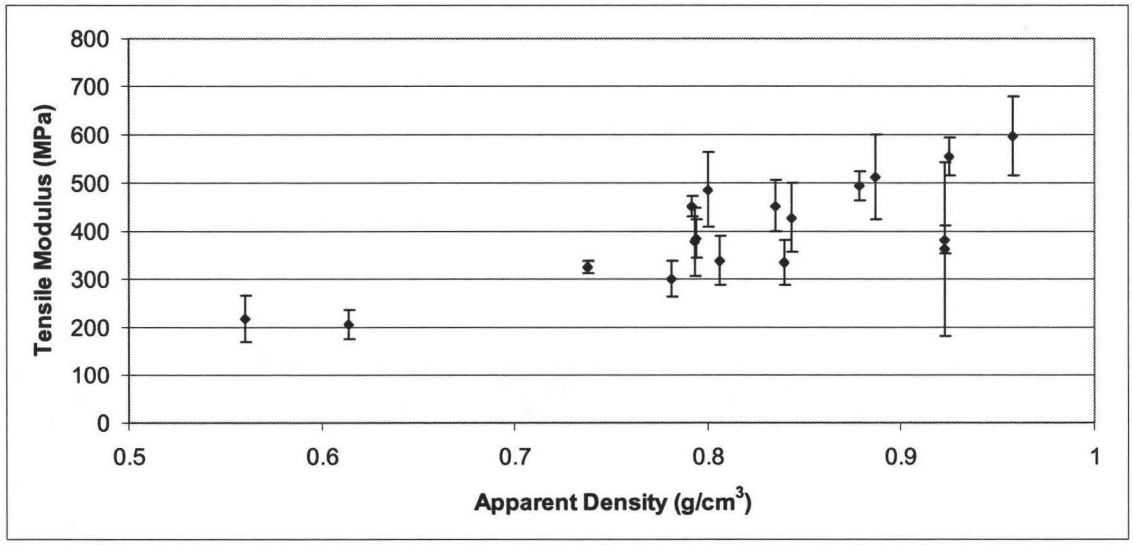

Figure 4.3.4: Comparison of density and tensile modulus for the TPO parts.

Applying a second-order polynomial regression to the tensile modulus/density data, a model can be established with a correlation coefficient (R^2) of 0.69, and an exponential value of 1.7331 (see Appendix III for ANOVA table). The second-order model was used because of the assumption that as density decreased, the cell diameter measurement of the gaseous cells increased at a second order rate (for derivation, see Appendix IV), and as the cell diameter decreases, the area to which the tensile force is applied decreases. The tensile modulus appeared to increase with apparent density. As with the tensile break strength data, the runs with solid cores had lower tensile moduli

than parts of similar apparent density. Again, this is likely a result of the skin/core interface which is the most likely location of crack propagation. For samples with solid cores, the weakest area within the parts is the interface, resulting in crack propagation occurring by delamination, while samples with foamed cores were more likely to distribute the stress within the foam. The foam can act as a crack arrestor, increasing the amount of potential stresses that can be applied to the system before failure occurs.

4.3.2 Flexural Modulus

The flexural modulus was measured for the 16 foam runs, and the 2 additional runs with solid core material as described in Chapter 3.

As observed in Figure 4.3.5[†], the flexural modulus values were statistically similar between test specimens cut close to the center and those close to the end of the plaque. The exceptions were Runs 9, 10, and 11 where the modulus for the specimen cut from the end of the plaque was noticeably higher. This indicates that the forces are more evenly distributed, in areas further from the injection point, indicating smaller cell sizes in this area.

[†] The flexural modulus for the samples cut from the end of the Run 3 plaques was impossible to measure, as the parts broke along the gap located along the center of the parts upon cutting.

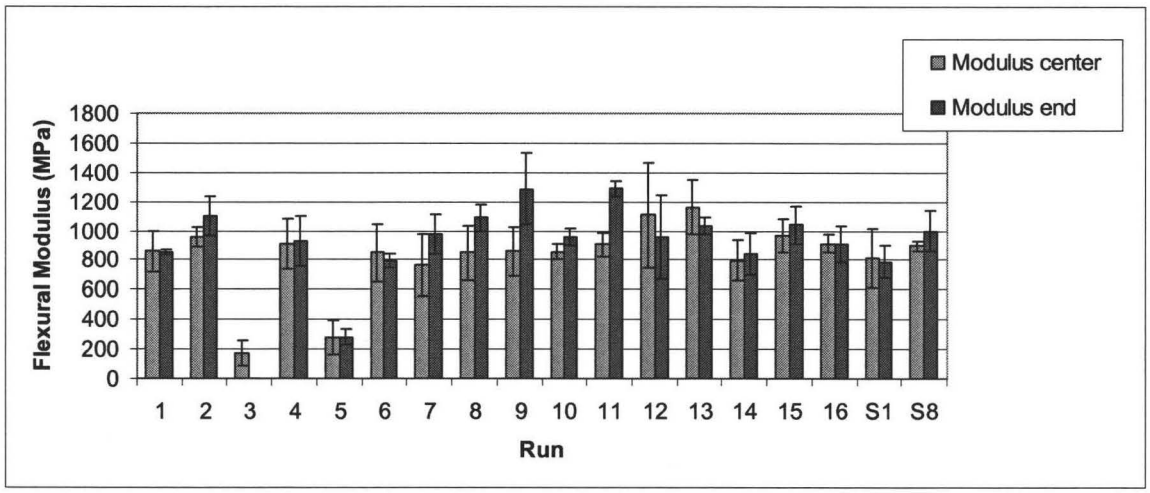

Figure 4.3.5: Comparison of flexural moduli TPO specimens. Examines samples punched close to the injection point, and close to the edge of the polymer plaques. (samples 1 and 8 are statistically the same as parts injected under the same conditions with solid cores, S1 and S8).

Similar to the other mechanical properties, it was observed that there was no statistical evidence of a decrease in the flexural modulus for Runs 1 and 8 compared to parts injected under the same conditions with solid cores (Runs S1 and S8). The flexural moduli were then compared to the density of the plaques, as displayed in Figure 4.3.6.

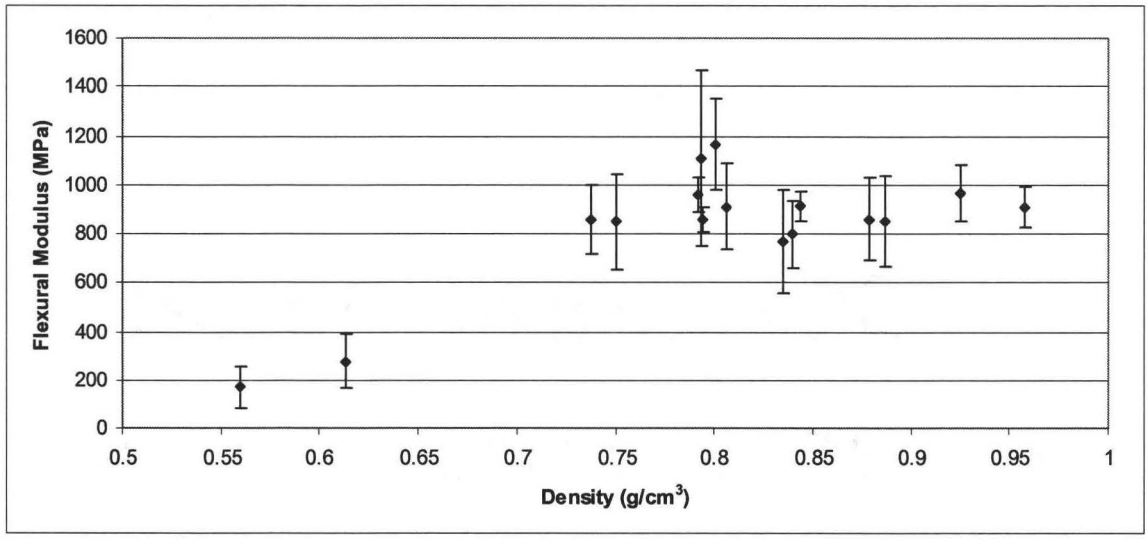

Figure 4.3.5: Comparison of flexural modulus and density of the TPO compounds.

The majority of samples were statistically similar in their measured flexural moduli except for the two distinctive samples with apparent densities of ~0.6 g/cm^3. However, there were additional two samples at ~0.8 g/cm^3 which had notably higher modulus values compared to the majority – these corresponded to Runs 12 and 13. The insensitivity of flexural modulus to foaming is seen as a positive outcome since it does not require the same amount of optimization as other factors would. A linear regression was used to determine main contributors, the results of which indicated that the *distance-to-cells* measurement was the main contributor to the variance in the flexural modulus (see AppendixI). Such a finding indicated that the majority of the flexural stresses were concentrated in the solid polymer. The foam takes a secondary role, possibly compressing and absorbing the force.

Runs 1 and 10 showed poor tensile properties, however, they show similar flexural properties as all samples with the exception of Runs 3 and 5. It appeared that the presence of a foamed core assisted in maintaining the flexural modulus of a specific sample, however, the planar separation was inadequate to maintain the modulus, likely compressing with the flexural force. It follows that the large cells easily compressed as well, since larger cells cannot transfer stress to as many locations within the specimen due to their size.

The similar mechanical properties between the plaques with solid cores and parts with foamed cores was consistent with a study completed by Kalfoglou (Kalfoglou, 1978), who examined the structure-properties relationship of composite films. The study showed mutual ductile reinforcement when rigid materials were layered with flexible materials. This could follow into a rigid foam and a flexible solid material, as

crystallization is less favorable in the foamed material due to the gaseous cells, causing a rigid core. The solid material was more likely to form crystalline material, increasing the flexibility of the material.

5.0 "The Main Four"

The purpose of this chapter was to, a) compare integral foams to co-injected parts with foam cores, and b) determine the effects of talc and nano-particles. One set of processing conditions, i.e. Run 1 from Chapter 4.0, were selected for these trials. The materials of examination included the formulation examined in Chapter 4 (i.e. 70vol% PP with 30vol% elastomer), as well as that same formulation blended with 20vol% (w/w) talc (TPOtalc) and finally a commercial-grade TPO nanocomposite from Basell (Basell

DX277AC). To address the issues posed above, each material mentioned was used in the creation of three different molded parts:

- Coinjection-molded foam - sample made from a foam core, and a solid skin injected from two separate streams (referred to as ***Run 1***).
- Integral-molded foam[‡] - using the conventional low-pressure method (short shot) to create foam using a single injection stream (referred to as ***Integral***). The shot size was comparable to that of a solid part
- Solid part – sample prepared by co-injection molding of the same material from two separate streams (referred to as ***S1***).
- Solid part – sample prepared from a single injection stream (referred to as ***Solid***)

The densities of Run 1, integral, S1 and solid for the three material types are listed in table 5.1.1.

Two additional runs were completed using the same parameters of co-injection of foamed material into a solid skin material using TPO as skin and TPOtalc as core (SCT), and TPOtalc as skin and TPO as core (STC).

Before discussing the physical measurements, a note should be made on the appearance of the molded parts based on co-injection versus integral foaming. The surface of the plaques which were processed using co-injection molding with a foamed core appeared visually the same as those of a solid part, showing a Class A surface, with the exception of the plaque composed of TPOtalc, which expanded in the gap direction, creating a part that was much wider in the gap direction than the desired mold shape,

[‡] See Appendix V for parameters of Integral and Solid injection molded parts.

likely due to a pressure buildup within the polymer part. The parts that were composed of integral foam showed a swirled appearance in areas very close to their corners, indicating that for larger molds, this method may not be sufficient as the material would be required to travel much farther in the mold than in our laboratory setting, and break-through from fountain flow could potentially occur.

5.1. Density

Apparent density was measured and compared for the different polymer parts as described in Chapter 3. The results are summarized in Figure 5.1.1. As observed, for all of the materials, the integral foam parts experienced the greatest decrease in density as compared to the solid parts, followed by the co-injected parts with a foamed core. The co-injected solid parts (S1) showed a decrease in density for the TPO and TPO talc parts when compared to solid single injection molded parts, which will be explained in more detail further in this chapter. The Basell parts showed very little decrease in density when foamed as opposed to a solid part. The reduction in apparent density from a single injection solid part for the three remaining types of processes are listed in Table 5.1.1.

The integral foam parts contained a swirl appearance, indicating gaseous cells reached the surface of the plaques, and then ruptured, creating open cells. This did not occur in the co-injection molded parts with foamed cores. Infact, the gaseous cells did not reach the skin/core interface as will be discussed in Section 5.2 of this chapter (the *distance-to-cells* measurement always is greater than the skin thickness measurement). This indicates that heat transferred differently in the co-injection molded parts and the integral foam parts. In the co-injection molded parts, heat was required to transfer

through a far less viscous, solid interface, while in the integral foam plaques, heat transfer was much faster because of the foamed material had a higher viscosity.

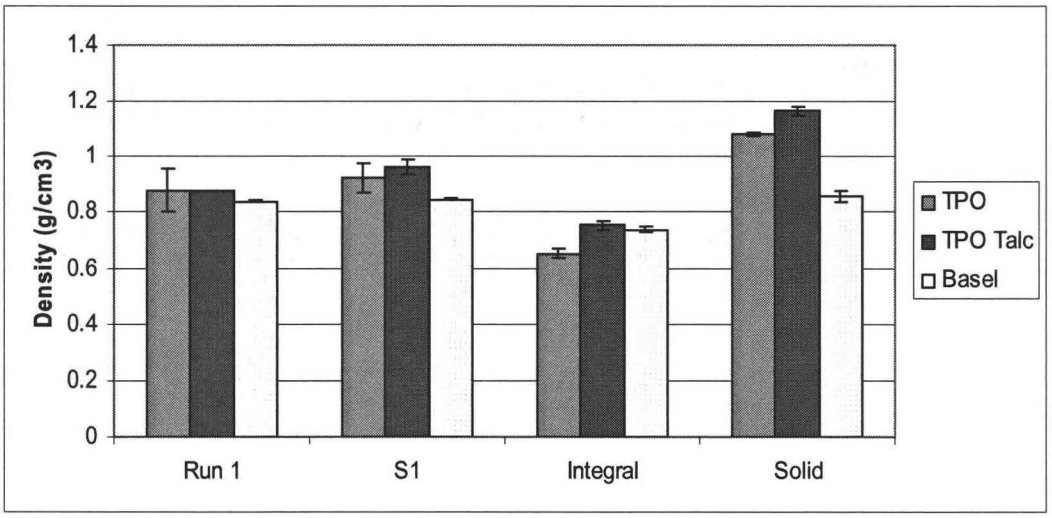

Figure 5.1.1: Comparison of the Main Four Apparent Densities. Graphed are injection molded parts for co-injection with a foamed core (Run 1), co-injection molding with a solid core (S1), an integral foam (Integral), and a solid injection molded part.

Table 5.1.1: Apparent density reductions from a solid single injection molded part for the three remaining processes examined§.

	Co-injection molded, foamed core	**Co-injection molded, solid core**	**Integral Foam**
TPO	19%	15%	40%
TPOtalc	24%	17%	35%
Basell	12 %	1 %	14%
SCT**	22%	X	X
STC	21%	X	X

Note the lower density of the *S1* parts versus the *Solid* parts for TPO and TPOtalc materials. This was because a larger mass of material was required to pack the mold when a single shot was made, as opposed to a co-injection shot. The TPO and TPOtalc

§ Maximum error of percentage apparent density decreases was 5%
** SCT and STC decreases were calculated using weighted average method discussed in Appendix I

materials likely experienced a pressure drop effecting the shear during the changeover between skin and core injection nozzles while the integral plate changed position (this lasted for less than a second). The pressure drop, however, likely allowed the material in the mold to relax slightly, allowing the free space volume to expand, while decreasing the volume available for more material to be injected, and supporting the observation that less material was required to pack the mold completely when co-injection was utilized as opposed to a single injection. Basell did not experience this effect. Likely, the momentary pause while the integral plate was changing over barrels was not enough to affect this material because it contained nanoclay filler. The amount injected was volume based.

Not included in the figure were the density values for the STC sample, $0.870 g/cm^3 \pm 0.005 g/cm^3$, and the density for the SCT sample, $0.91 g/cm^3 \pm 0.02 g/cm^3$. The densities of the STC and SCT samples appeared to be reasonable, as the density of TPOtalc was slightly higher than that of TPO. Considering the SCT sample had a higher density than the STC sample, TPOtalc material, (TPOtalc had a greater density than the TPO compound), composed the core of the SCT part, which was 85vol% of the injected material .

5.2. Microscope Observation

In order to better understand the density results, the cellular structures of the plaques were examined. The plaques were studied as in Chapter 4.0 to better clarify variances and trends in the density and the mechanical properties of the parts.

5.2.1. Cell Size

Average cell size was examined along the flow plane of the S1 and integral foam parts. Small error in cell size indicated little variance in the cell size along the path of flow, while larger error indicated that the cell sizes changed slightly with flow, as observed in Figure 5.2.1.

The co-injection TPOtalc parts with foamed cores experienced a slight planar separation in the gap direction similar to Runs 3 and 5 in Chapter 4, Section 4.2.1. The inclusion of talc in TPOtalc increased the amount of nucleation and the viscosity when compared to TPO parts. The viscosity increase likely led to a larger degree of viscous heating in the TPOtalc as opposed to the TPO material, so cooling occurred over a longer period of time. The slow cooling resulted in gaseous cells experiencing an exaggerated coalescence along the center of the gap in these parts, causing center separation of the TPOtalc parts.

It should be noted that all foamed samples in the group contained cells that were all circular in shape, not elliptical, indicating that cell nucleation and growth did not occur during flow.

The STC and SCT parts did not experience the same heat transfer that the TPOtalc parts did. This is likely a result of the TPO material without talc, which was slightly less viscous than the TPOtalc[††], resulting in less viscous heating.

[††] MFI measurement of the TPO was 9.7±0.2g/10min , while the MFI measurement of TPOtalc was 9.20±0.2g/10min, run at 230°C under a 10kg weight.

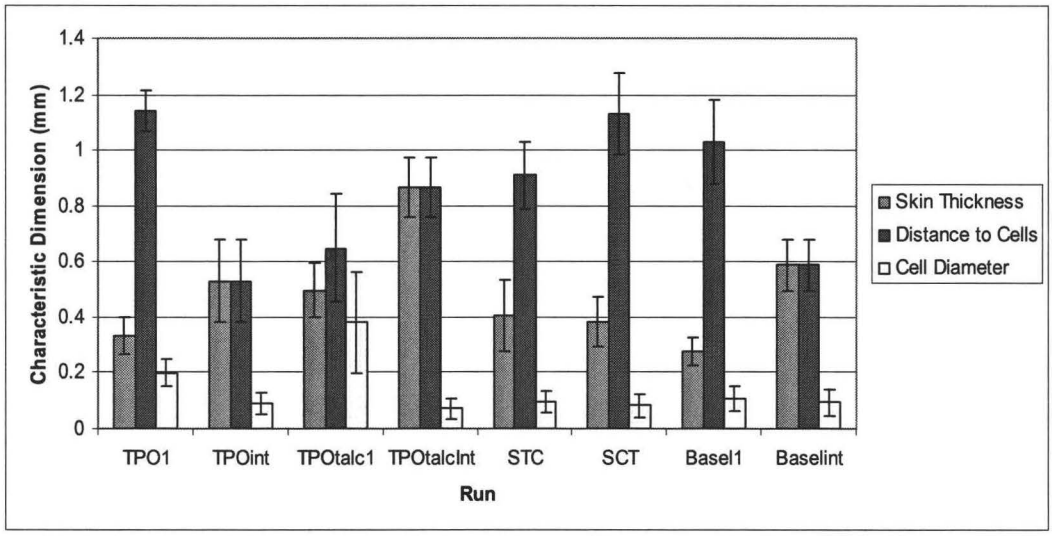

Figure 5.2.1: Comparison of microscope data of Main Four. Examined are skin thickness, distances to cells, and the cell diameters of the integral foam (suffix 'int'), and co-injected plaques with foamed core material (suffix '1').

5.2.2. Skin Thickness and Distance to Cells

Skin thickness and distance-to-cells were the other indicators measured to analyze how well the gaseous cells distributed throughout the plaques in the gap direction. Skin thickness and distance to cells are the same value for integral foams since there was no solid material injected prior to injection of the foam material. To clarify, the skin thickness in co-injected parts was considered to be the "skin" material layer, while the *distance-to-cells* measurement was self explanatory; the measurements were the same as discussed in Chapter 4. Larger variance for the given error of a quoted value indicated greater change in the property at the injection point in comparison to the end of the mold. The change in the *distance-to-cells* measurement along the flow plane of the part indicated a possible change in mechanical properties in localized areas of the injection molded sample, and possibly little or no foamed material in the gap direction at given distances from the injection point.

As with the TPO samples examined in Chapter 4.0, the skin thicknesses were consistent among the co-injection parts, as seen in Figure 5.2.1, due to the volume of skin being held constant during processing. The *distance-to-the cells* measurement was higher for co-injected molded parts with foamed cores than for integral foams for all the samples except for the TPOtalc material, indicting that cells concentrated at the center of the parts while the cell growth and plaque cooling stages were occurring.

In the case of TPOtalc, the *distance-to-the cells* measurement was greater for the integral foam than the co-injection molded part. This was possibly a result of the greater number of nucleating sites resulting from the amount of talc in the sample combined with the blowing agent that are contained in the integral foam sample, as the co-injection molded part had the solid skin. It follows that the foamed TPOtalc transferred heat less efficiently than its solid counterpart due to the gaseous cells. The slower heat transfer could have caused the gaseous cells to be concentrated along the center of the polymer plaque which again indicates that the viscous heating increased the amount of time spent in the nucleation and cell growth stages of foaming for these parts, as in Runs 3 and 5 in Chapter 4.

The *distance-to-cells* measurement of the integral foamed plaques for the TPO and the Basell material were less than those of the co-injection molded plaques. Heat transfer through the solid skin was likely hindered for the co-injection molded parts with foamed cores, resulting in extended time in the cell growth stage. The TPO material showed this more effectively than the Basell plaques, as the cells are much larger for the co-injection molded part with foamed core.

STC and SCT had *distance-to-cells* measurements were consistent with the skin material used in each sample (when entire sample was composed of the same material). STC had a similar measurement to the TPOtalc material, while SCT had a measurement similar to the TPO material. This again indicated that heat transfer was crucial in determining the amount of time the system remains in the bubble growth stage of foaming and hence the pattern in which the cells are dispersed in the gap direction.

Heat transfer of the material appears to greatly effect the foam morphology of each part examined. Multiple factors could have altered these properties; it appeared that additives can made great differences when processing foams.

5.3 Mechanical Properties

The ultimate tensile strength, tensile moduli and flexural moduli were measured for the plaques. Comparisons were made to determine if co-injection molding a foam was a reasonable alternative to integral foaming. As in Chapter 4.0, this is a question of tradeoffs, as will be observed in the following Section.

First, the tensile modulus was examined and compared to the density of each of the plaques (see Figure 5.3.1).

The Basell samples showed very small change between different types of injection molding. In fact, the only notable change was in the density of the integral foamed part, which was lower than the solid and co-injection versions of this material. This was likely a result of the small gaseous cells, which were consistent with literature review findings.

Again, a linear relationship between the tensile modulus and apparent density of the TPO material was observed. The TPOtalc showed an expected decrease in tensile modulus for the co-injected parts with a foamed core due to the center separation, constant with the observations of Runs 3 and 5 examined in Chapter 4, which had planar separation. The integral case for the TPOtalc parts appeared to have a higher tensile modulus than the co-injection molded version containing a foamed core.

The moduli of the STC and SCT parts are in the range of the co-injected parts composed of the same material, which was expected. They are very similar to the co-injection molded parts composed of TPO, with both a foamed core and a solid core. Referring to the morphological measurements, the STC and SCT were very similar dimensionally to the co-injection molded TPO and TPOtalc parts. It is interesting to note that mechanical properties appeared consistent with the TPO solid parts.

Next, the flexural modulus was measured for the plaques (see Figure 5.3.2).

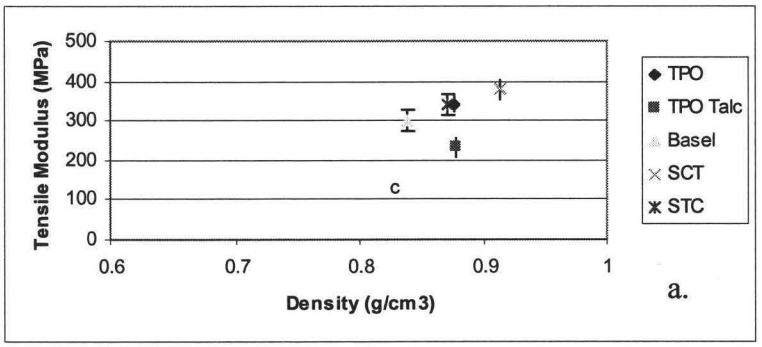

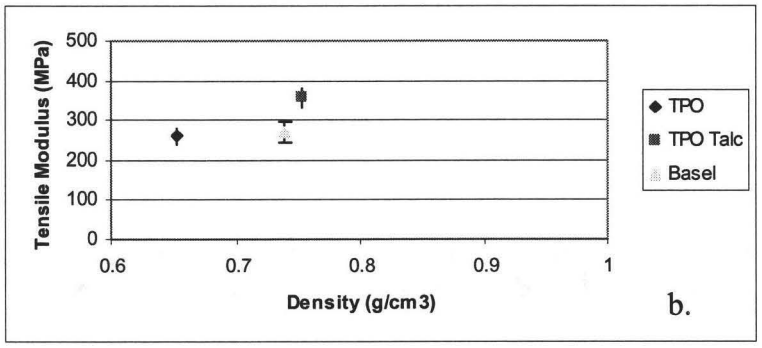

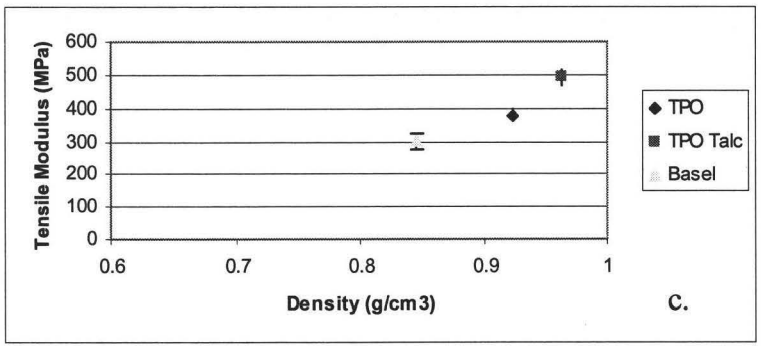

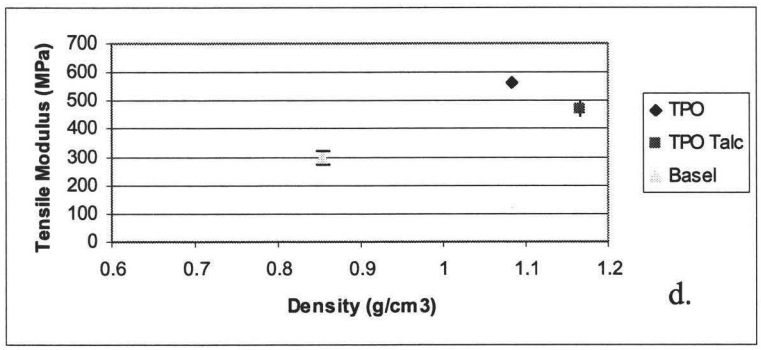

Figure 5.3.1: Tensile modulus versus apparent density for Main Four a.) Co-injection molded parts with foamed cores, b.) Co-injection molded parts with solid cores, c.) Integral foams, d.) Solid single injection molded parts.

The TPO samples show notably lower flexural modulus values for the co-injection molded parts, which indicated that for these samples the interface is the source of fracture, rather than the foam. The interface is likely the source of fracture because the co-injection molded parts for TPO with solid core and the foamed core had statistically the same flexural modulus, indicating that fracture initiated in an area that was mechanically weak and common to both, i.e. the skin/core interface.

The TPO with talc appeared to have the same flexural moduli regardless of production process, as did the Basell parts, indicating that deformation was not within the foamed material, or the skin/core interface in co-injection. It was assumed that the additives affected the tensile results, as the TPO material showed greater variances in the flexural moduli of it's main four, and contained no additives.

Next, the tensile break strength of the parts was examined, which can be viewed in Figure 5.3.3

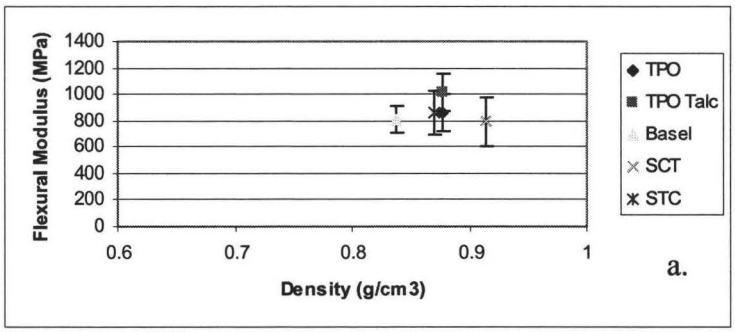

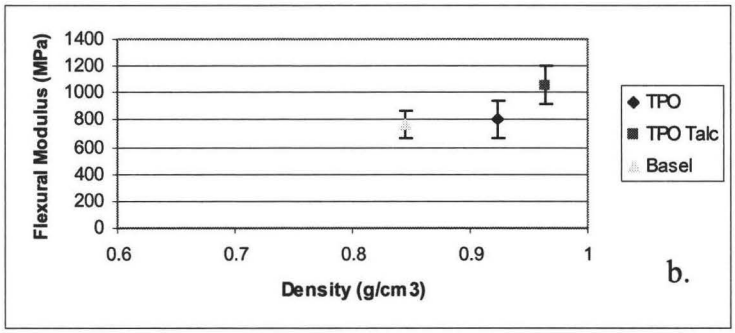

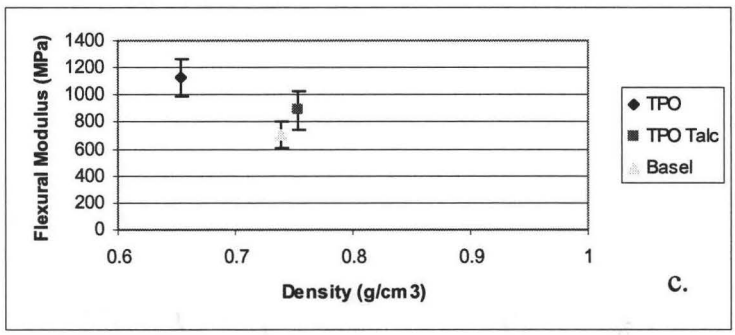

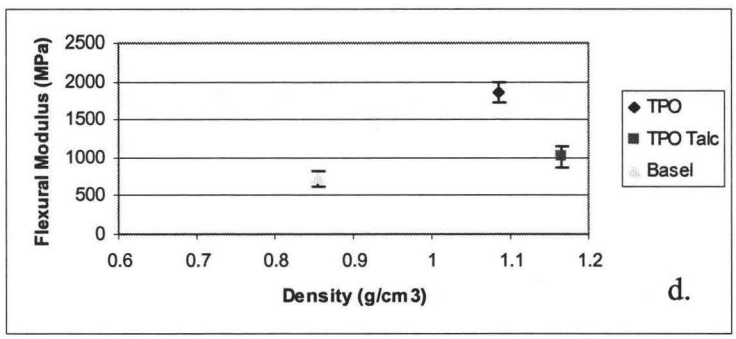

Figure 5.3.2: The flexural moduli versus density for Main Four a.) Co-injection molded parts with foamed cores, b.) Co-injection molded parts with solid cores, c.) Integral foams, d.) Solid single injection molded parts.

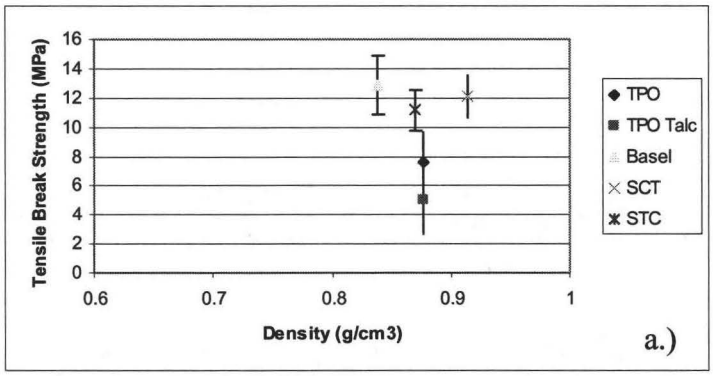

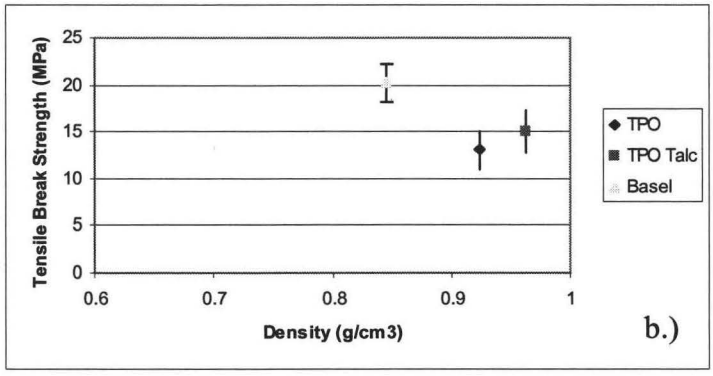

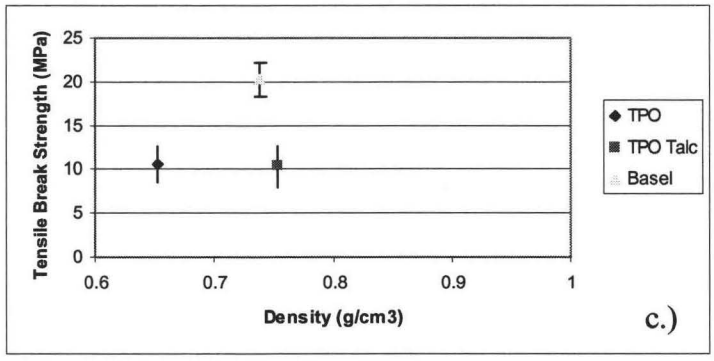

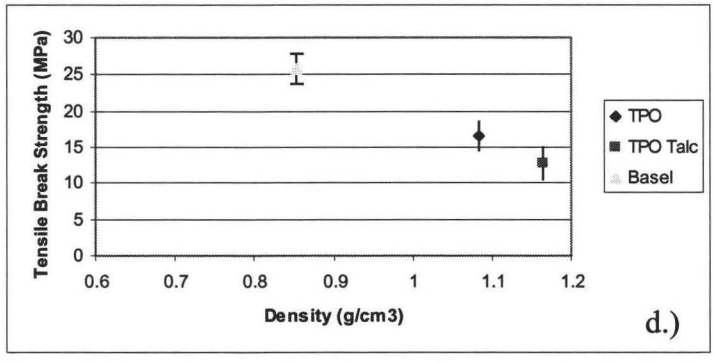

Figure 5.3.3: The tensile break strength compared with density for Main Four a.) Co-injection molded parts with foamed cores, b.) Co-injection molded parts with solid cores, c.) Integral foams, d.) Solid single injection molded parts.

All samples show similar patterns, indicating that the co-injection molded parts with a foam core had the lowest tensile break strength of the four runs for the three types of material. Because the co-injection molded samples with foamed cores showed relatively low break strengths, it is assumed that failure initiated within the structure. For the co-injection molded parts with foamed cores, the gaseous cells were concentrated along the center in the gap direction, perhaps allowing the part to act as two separate, thin layers, rather than one solid part, or a plane slip. The Basell material integral foam and the co-injection molded part with a solid core showed the same amount of break strength, which indicated that fracture could have initiated within the foamed material or at the skin/core interface, however, when these two factors were combined, the break strength greatly decreases for this material, however with the analysis completed on these parts, it was impossible to determine where failure occurred first.

A statistical regression analysis was completed to relate the morphologies to the mechanical properties examined in this Section (see Appendix I). Results indicated that the *distance-to-cells* measurement was the most important factor in density reduction, flexural modulus, and tensile modulus properties. The error was too great to determine any relation to the tensile break strength, indicating that the values examined did not relate to the tensile break strength.

In order to further examine the co-injection molded parts, the STC and SCT samples were examined, as observed in table 5.3.1. The interface between the skin and core was innately weaker then when the same material was used for the skin and core. The STC sample (containing TPOtalc in the skin, and TPO in the talc), had higher mechanical properties, and lower density than the SCT sample.

Table 5.3.1: Comparison of mechanical properties of the STC and SCT samples.

	Tensile Modulus (MPa)	Tensile Break Strength (MPa)	Flexural Modulus (MPa)	Density (g/cm^3)
STC	380±30	12 ±1	1000±100	0.870±0.005
SCT	340±20	11±1	800±100	0.91±0.02

As would be expected, the core material which comprised 85% of the part dominated when assuming a rule of additivity; however, this was not the case for the STC and SCT samples (except, of course, in the case of density). The SCT sample contained a greater amount of the TPOtalc material, which regularly showed higher values of mechanical properties as observed in Figures 5.3.1, 5.3.2, and 5.3.3, however, the STC material which contained a greater amount of the TPO material showed higher values in mechanical properties. It appears that the mechanical properties were statistically the same for the SCT and SCT values, except that the STC contained a lower density due to the larger amount of less dense material within the sample. Also observed in Figures 5.3.1-5.3.3, the SCT and SCT samples have comparable mechanical properties to co-injection molded parts containing the same TPO or TPOtalc material within the skin and the core.

5.4 Discussion

It was apparent that the distribution of the cells within the plaques had the greatest influence on the tensile strength and density of the parts, while the skin thickness had the greatest influence on the flexural modulus and break strength of the parts. When the skin was the greatest influence on the parts, the foam structure and location were secondary

factors, and likely not the location site of initiation of the failure for the particular property.

The addition of talc to the TPO was to increase stiffness of the part, as well as create more nucleating sites for gaseous cells to form during processing. The density of the material increased slightly (see Figure 5.1.1), and observations showed that mechanical properties were statistically the same for most measurements. As was observed in the co-injection molded TPO and TPOtalc parts, the foaming was excessive when the talc was contained in the TPO. This did not occur in the SCT and STC samples, which indicated that the talc in the skin material hindered heat transfer of the part, causing cell nucleation to occur for a greater amount of time than the TPO material, and that the excessive cell nucleation only occurred when there were additional nucleation sites present because of the talc material, and the heat transfer was restricted.

In the parts where the *distance-to-cells* measurement had the greatest influence, it was likely that the fracture initiated within the foam. For the tensile samples, the foam likely helped maintain the modulus, while the break strength relied on the skin structure. Fracture likely occurred within the core structure; however, the final break value was a result of the skin structure for these tensile samples.

For the flexural testing, it appeared that effects relied mainly on the skin thickness from the statistical analysis, as well as the similar flexural moduli examined in Chapter 4.

Chapter 6. Conclusions

Co-injection molding is a worthwhile option in the automotive industry, after consideration of the observations of this work.

Density can be reduced, and it appears that there is an optimum level for which this can be done. There is a direct trade off in mechanical properties, and in situations such as the Basell material, they were not worth the extra material costs. The TPO and TPO talc, however, do show promise in this area, and led to the conclusion that the material itself played great bearing as to whether or not this process should be used.

An interesting observation that was made between the selected experiments was that in all cases, co-injection molding with a solid core reduced the density of the part when compared to a single injection of solid material due to a pause in the process which

allow for the material to "relax" during the injection cycle. In the TPOtalc experiments, the solid parts and the co-injection molded parts with solid cores behaved similarly in mechanical testing. This method is a likely alternative for new machines in this field, with foaming in the core material, or a cheaper core material mixed with a compatibliser. Recycled materials can also be used as the core material, and virgin material can be used as the skin material.

This study produced excellent results, showing an apparent density decrease of up to 32.0% ± 0.8% with only minor decreases in mechanical properties, while maintaining a Class A surface.

References

Bogaerds ACB, M.A. Hulsen, G.W.M. Peters, and F.P.T. Baaijens, "Stability analysis of IM flows," Journal of Rheology **48**(4), 765-785 (2004).

Bravo, V.L., and A.N. Hrymak "Nozzle injection of physical blowing agents in the injection molding of microcellular foams" Int. Pol. Proc. **20**(2), 149-156 (2005).

Chen, L., H. Sheth, H., and R. Kim, "Effect of Filler Size on Cell Nucleation during Foaming Process," Polymer Engineering and Science **41**, 990-997 (2001).

Chen, L., X. Wang, R. Straff, and K. Blizard, "Shear stress nucleation in microcellular foaming process," Polymer Engineering and Science **42**(6), 1151-1158 (2002).

Chen SC, N.T. Chen, K.S. Hsu, and K.F. Hsu, "Study of polymer melt flow in sequential injection molding process," AIChE Journal **42**(6), 1706-1714 (1996).

Doroudiani S, C.B. Park, and M.T. Kortschot "Effect of the crystallinity and morphology on the microcellular foam structure of semicrystalline polymers" Polymer Engineering and Science **36**(21) 2645-2662 (1996).

Gong, S., M. Yuan, A. Chandra, H. Kharbas, A. Osorio, and L.S. Turng "Microcellular Injection Molding" Int. Pol. Proc. **20**(2), 202-214 (2005).

Gosselin, R., and D. Rodrigue "Cell Morphology Analysis of High Density Polymer Foams," Polymer Testing **24**, 1027-1035 (2005).

Jancar J, and A.T. Dibenedetto, "The mechanical properties of ternary composites of polypropylene with inorganic fillers and elastomer inclusions," Journal of Materials Science **29**, 4651-4658 (1994).

Kalfoglou, N.K., "Effect of fillers on the compatibility of polymer blends," Journal of Applied Polymer Science **22**, 989-997 (1978).

Keestra, B.J., P.D. Anderson, and H.E.H. Meijer "Two component injection molding of phase separating blends" Intern. Pol. Pro. **21**(2), 168-174 (2006).

Kramschuster, A., R. Cavitt, D. Ermer, Z. Chen, and L.S. Turng. "Quantitative Study of shrinkage and warpage behavior for microcellular and conventional injection molding," Polymer Engineering and Science, **45,** 1408-1418 (2005).

Leduc, S. and D. Rodrigue, "Effect of Weld Lines on the Injection Moulding of Structural Foams. I. Foam Morphology," Cellular Polymers **24**(6), 313-327 (2005).

Lee, H., P.D. Fasulo, W.R. Rodgers, and D.R. Paul, "TPO based nanocomposites. Part 1. Morphology and mechanical properties" Polymer. **46**(25), 11673-11689 (2005).

Lee, L.J, C. Zeng, X. Cao, X. Han, Jiong Shen, and G. Xu "Polymer nanocomposite foams" Composites Science and Technology **65**, 2344-2363 (2005).

Li, C.T. and A.I. Isayev "Interface development and encapsulation in simultaneous co injection molding. I. Two-Dimensional modeling and formulation" Journal of Applied Polymer Science **88**, 2300-2309 (2003).

Mavridis H., A.N. Hrymak, and J. Vlachopoulos, "Finite element simulation of fountain flow in Injection Molding" Polymer Engineering and Science **26**(7), 449-454 (1986).

Naguib H.E., C.B Park, U. Panzer, and N. Reichelt "Strategies for Achieving Ultra Low-Density Polypropylene Foams" Polymer Engineering and Science **42**(7), 1481-1492 (2002).

Naguib HE, Park CB, and Song S "Effect of supercritical gas on crystallization of linear and branched PP resins with foaming additives" *Ind. Eng. Chem. Res.***44**, 6685-6691 (2005).

Park, C.B., and L.K Cheung, "A Study of cell nucleation in the extrusion of polypropylene foams," Polymer Engineering and Science, **37**(1), 1-10 (1997).

Qin, X., M.R. Thompson, A.N. Hrymak, and A. Torres "Rheological Comparison of Chemical and Physical Blowing Agents in a Thermoplastic Polyolefin" Ind. Eng. Chem. Res. **45**, 2734-2740 (2006).

Shen, C., A. Kramschuster, D Ermer, and LS Turng "Study of Shrinkage and Warpage in microcellular co-injection molding," Intern. Pol. Proc **21**(4), 393-401 (2006).

Simha, R. and P. Moulinie, "Statistical Thermodynamics of Gas Solubility in Polymers" in "Foam Extrusion: Principles and Practice," S,-T. Lee Ed., Technomic Publishing Co., Lancaster, PA (2000), pp. 15-20.

Sun X., H. Liu, G. Li, X. Liao, and J. He "Investigation on the cell nucleation and cell growth in microcellular foaming by means of temperature quenching" Journal of Applied Polymer Science **93**, 163-171 (2004).

Taki, K., K. Tabata, S. Kihara, and M. Ohshima "Bubble coalescence in foaming process of polymers," Polymer Engineering and Science, **46**(5) 680-690 (2006).

Tatibouet, J, R. Gendron,, A. Hamel, and A. Sahnoune, "Effect of Different Nucleating Agents on the Degassing Conditions as Measured by Ultrasonic Sensors," Journal of Cellular Plastics, **38,** 204 (2002).

Throne, J.L. "Thermoplastic Foam Extrusion," Hanser Gardiner Publications, Cincinnati, Ohio (2004).

Turng, L.S. and H. Kharbas "Development of a Hybrid Solid-Microcellular Co-injection Molding Process" Intern. Pol. Pro. **19**(1), 77-86 (2004).

Villamizar, C.A. and C. Dae Han "Studies on structural foam processing II. Bubble dynamics in foam injection molding," Polymer Engineering and Science **18**(9), 669-710 (1978).

Watanabe, D., U.S. Ishiaku, T. Nagaoka, K. Tomari, and H. Hamada. "Flow behaviour of sandwich IM in sequential and simultaneous injection" Intern. Pol. Pro. **18** (2), 199-203 (2003).

Xanthos, M., S.K. Dey, "Foam Extrusion of Polyethylene Terephthalate (PET)" in "Foam Extrusion: Principles and Practice," S,-T. Lee Ed., Technomic Publishing Co., Lancaster, PA (2000), pp. 331-333.

Zhou, Q., WeiPing, G., Wu, J., Wang, J., Zhen, H.Y., Wu, Q. "Compound Mechanism of the Endo-Exothermic and Exo-Endothermic ± Balanced Blowing Agent" Journal of Cellular Plastics, **36**(2), 126 (2000).

Appendix I

A simple linear regression was completed using:

$$\hat{y} = \hat{\beta}\,\hat{\chi} + \hat{e} \qquad (1)$$

The y matrix included the measurement of interest, and the χ matrix contained the parameters used from the DOE. The β and e matrices were calculated using a linear regression.

Since the β values were not proportional to the input values, each was multiplied by the average value of the parameter it referred to (for instance, the β parameter that referred to the injection temperature of the skin material was multiplied by 210, the average of the two input levels used in the DOE).

Once the β values were proportioned, they were compared. The parameters with the largest absolute values were considered to have the greatest influence on the measurement of interest. Any proportioned parameters that had an absolute value less than the calculated error showed no statistical evidence of affecting the measured parameter for the range of values studied.

This method was used for the density values of the TPO without talc material. The following table lists the results:

DENSITY	β	χ	B proportioned
Skin Temperature	0.0019792	210	0.415632
Core Temperature	-0.0022508	210	-0.472668
Injection Speed 1	-0.00044782	80	-0.0358256
Injection Speed 2	-0.0013129	80	-0.105032
Injection Speed 3	-0.00019572	80	-0.0156576
Hold Time	0.0028517	17	0.0484789
Percent Core	0.013276	77	1.022252
Mold Temperature	0.00027141	50	0.0135705
Conc. Foaming Agent	-0.025313	3	-0.075939
		Total	0.7948112
		Error	3.08%

The same method was used to design linear equations relating the skin thickness, *distance-to-cells* measurement, and the cell size to the density, tensile break strength, tensile modulus, and flexural modulus for the TPO without talc parts to determine what morphological properties had the greatest influence on the mechanical properties.

			BETA			PROPORTIONED	
	Avg measurement	Tensile Break Strength	Tensile Modulus	Flexural Modulus	Tensile Break Strength	Tensile Modulus	Flexural Modulus
Skin Thickness	0.345853734	15.206	-1319	2773.6	5.259051883	-456.1810754	959.2599172
Distance to cells	0.781919973	-3.3181	42.358	-43.313	-2.594488661	33.1205662	-33.86729977
Cell Diameter	0.172134832	-19.361	-440.6	148.18	-3.332702477	-75.84260685	25.50693936
Density	0.802897479	19.367	1125.9	-47.368	15.54971548	903.9822719	-38.0316478
				Total	14.88157623	405.0791558	912.867909
				Error	9.9775	173.5	376.27

Again, this method was used to design linear equations relating the skin thickness, *distance-to-cells* measurement, and the cell size to the density, tensile break strength, tensile modulus, and flexural modulus for the "Main Four" foamed parts.

The β values for the mechanical properties were:

	Tensile Modulus	**Tensile Brk. Str**	**Flex Modulus**	**Density**
Skin Thickness	193.75	13.312	754.04	0.34255
Distance to cells	261.59	7.436	405	0.61602
Cell Diameter	-66.4	-14.245	1090.3	0.80915

The X values for the observed morpological measurements were:

Skin Thickness	0.48425542
Distance to cells	0.8549406
Cell Diameter	0.13994524

And finally, the proportioned β values for the mechanical properties were:

	Tensile Modulus	**Tensile Brk. Str**	**Flex Modulus**	**Density**
Skin Thickness	93.8244871	6.44640811	365.147955	0.165882
Distance to cells	223.64391	6.35733827	346.250941	0.526661
Cell Diameter	-9.2923638	-1.9935199	152.582294	0.113237
Error	75.707	11.476	485.52	0.088223

Appendix II

Data observed and compared for the TPO without talc parts for Runs 1-16.

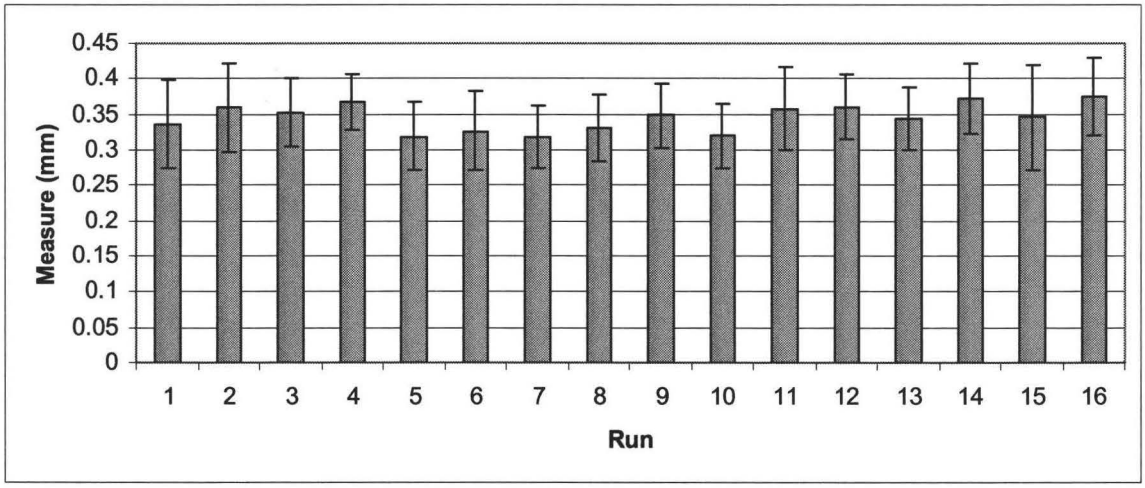

Average skin thicknesses of TPO without talc runs.

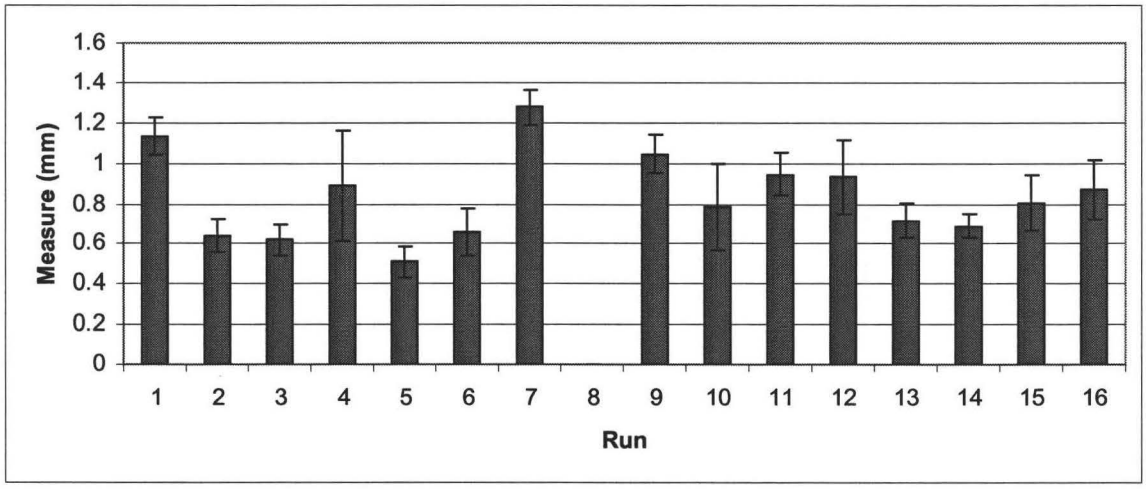

Average Distance-to-cells measurement for the TPO without talc runs.

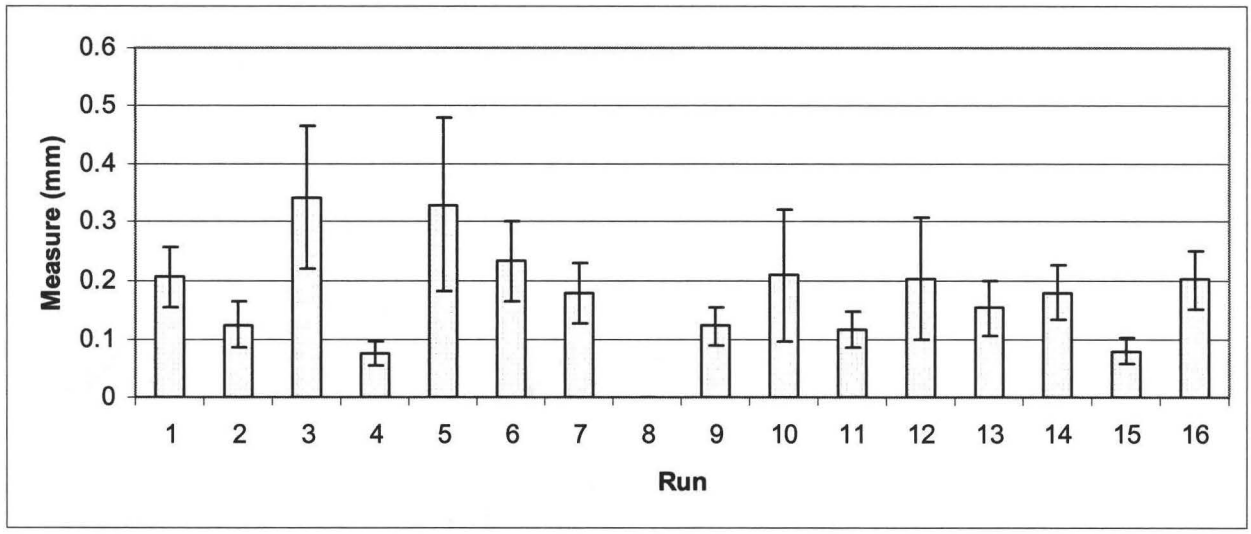

Average cell diameter for the TPO without talc runs.

Appendix III

ANOVA

	df	*SS*	*MS*	*F*
Regression	14	49798.03	3557.002	57.37101
Residual	1	62	62	
Total	15	49860.03		

$f_0 > f_{0.05}$, therefore we accept this value

Appendix IV

The entire mass of the plaques (m_T) was the sum of the mass of the cells (m_c), and the mass of the polymer material (m_P):

$$m_T = m_c + m_P \tag{A.1}$$

The mass of the cells is negligible, and mass is equivalent to the product of volume and density.

$$m_T = m_P$$

$$m = \rho V$$

$$m_T = \rho_T V_T \qquad \text{(A.2, A.3,A.4, A.5)}$$

$$m_P = \rho_P V_P$$

Substituting,

$$\rho_T V_T = \rho_P V_P \tag{A.6}$$

The volume of polymer is equal to the difference between the total volume (unchanging), and the volume of the cells (changes with the total density).

$$V_P = V_T - V_c$$

$$\therefore \rho_T V_T = \rho_P V_T - \rho_P V_c \qquad \text{(A.7, A.8)}$$

Since the total volume and the density of the polymer do not change:

$$\rho_T \propto -V_c \tag{A.9}$$

The cells are circular and elliptical, and relate to volume using a second order relationship.